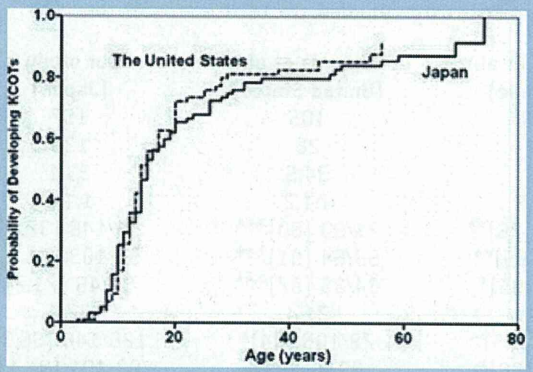

FIG. 4. A Kaplan–Meier curve of the risk of NBCCS patients developing KCOT at different ages; Japanese versus Americans. The data for Americans were derived from the previous report [Kimonis et al., 1997].

medulloblastoma is low in NBCCS, careful investigation is still required in young NBCCS patients since medulloblastoma is one of the most malignant tumors that can develop in NBCCS patients [Evans et al., 1991], and radiation therapy for medulloblastoma might cause subsequent BCC in the irradiated skin area [Smucker and Smith, 2006]. The incidences of other tumors; that is, ovarian and cardiac fibromas, are also similar to those in Western countries.

The estimated prevalence of NBCCS in the Japanese population was 1/235,800, which was lower than those reported in the United Kingdom (1/55,600) [Evans et al., 1993] and Australia (1/164,000) [Shanley et al., 1994]. However, since a considerable fraction of NBCCS patients are treated at local dermatologists or dentists, this estimate represents a minimum figure.

In conclusion, we investigated the clinical manifestations of 157 Japanese NBCCS patients and found a low frequency of BCC compared with those in the United States, Australia, and the United Kingdom. Our data suggest that Asian ethnicity and/or geographical factors play a pivotal role in the occurrence of BCC. Therefore, in Asia, a different strategy should be adopted for the management and treatment of NBCCS.

ACKNOWLEDGMENTS

We would like to thank Dr. Kazuma Noguchi, Dr. Hideki Uchikawa, Dr. Tadashi Shiohama, Dr. Maiko Suyama, and Dr. Hiromi Mizuochi, who helped with the NBCCS evaluation in this study. We are also grateful to the participating families and many cooperative doctors in Japan, whose contributions made this study possible. This research project was supported by the Ministry of Health, Labour and Welfare on Science Research Grants for intractable diseases in Japan (H22-intractable diseases-120).

REFERENCES

Ahn SG, Lim YS, Kim DK, Kim SG, Lee SH, Yoon JH. 2004. Nevoid basal cell carcinoma syndrome: A retrospective analysis of 33 affected Korean individuals. Int J Oral Maxillofac Surg 33:458–462.

Amlashi SF, Riffaud L, Brassier G, Morandi X. 2003. Nevoid basal cell carcinoma syndrome: Relation with desmoplastic medulloblastoma in infancy. A population-based study and review of the literature. Cancer 98:618–624.

Dessinioti C, Antoniou C, Katsambas A, Stratigos AJ. 2010. Basal cell carcinoma; What's new under the sun. Photochem Photobiol 86: 481–491.

Epstein EH. 2008. Basal cell carcinomas: Attack of the hedgehog. Nat Rev Cancer 8:743–754.

Evans DG, Farndon PA, Burnell LD, Gattamaneni HR, Birch JM. 1991. The incidence of Gorlin syndrome in 173 consecutive cases of medulloblastoma. Br J Cancer 64:959–961.

Evans DG, Ladusans EJ, Rimmer S, Burnell LD, Thakker N, Farndon PA. 1993. Complications of the naevoid basal cell carcinoma syndrome: Results of a population based study. J Med Genet 30:460–464.

Fujii K, Kohno Y, Sugita K, Nakamura M, Moroi Y, Urabe K, Furue M, Yamada M, Miyashita T. 2003. Mutations in the human homologue of *Drosophila patched* in Japanese nevoid basal cell carcinoma syndrome patients. Hum Mutat 21:451–452.

Gailani MR, Stahle-Backdahl M, Leffell DJ, Glynn M, Zaphiropoulos PG, Pressman C, Undén AB, Dean M, Brash DE, Bale AE, Toftgård R. 1996. The role of the human homologue of Drosophila patched in sporadic basal cell carcinomas. Nat Genet 14:78–81.

Gorlin RJ. 1987. Nevoid basal-cell carcinoma syndrome. Medicine (Baltimore) 66:98–113.

Gorlin RJ, Goltz RW. 1960. Multiple nevoid basal-cell epitheliomas, jaw cysts and bifid rib. A syndrome. N Engl J Med 262:908–912.

Hahn H, Wicking C, Zaphiropoulous PG, Gailani MR, Shanley S, Chidambaram A, Vorechovsky I, Holmberg E, Unden AB, Gillies S, Negus K, Smyth I, Pressman C, Leffell DJ, Gerrard B, Goldstein AM, Dean M, Toftgard R, Chenevix-Trench G, Wainwright B, Bale AE. 1996. Mutations of the human homolog of Drosophila patched in the nevoid basal cell carcinoma syndrome. Cell 85:841–851.

Hannuksela-Svahn A, Pukkala E, Karvonen J. 1995. Basal cell skin carcinoma and other nonmelanoma skin cancers in Finland from 1956 through 1995. Arch Dermatol 135:781–786.

Johnson RL, Rothman AL, Xie J, Goodrich LV, Bare JW, Bonifas JM, Quinn AG, Myers RM, Cox DR, Epstein EH Jr, Scott MP. 1996. Human homolog of patched, a candidate gene for the basal cell nevus syndrome. Science 272:1668–1671.

Jones EA, Sajid MI, Shenton A, Evans DG. 2011. Basal cell carcinomas in Gorlin syndrome: A review of 202 patients. J Skin Cancer 2011: 217378.

Kimonis VE, Goldstein AM, Pastakia B, Yang ML, Kase R, DiGiovanna JJ, Bale AE, Bale SJ. 1997. Clinical manifestations in 105 persons with nevoid basal cell carcinoma syndrome. Am J Med Genet 69:299–308.

Leiter U, Garbe C. 2008. Epidemiology of melanoma and nonmelanoma skin cancer—The role of sunlight. Adv Exp Med Biol 624:89–103.

Lindström E, Shimokawa T, Toftgard R, Zaphiropoulos PG. 2006. PTCH mutations: Distribution and analyses. Hum Mutat 27:215–219.

Madras J, Lapointe H. 2008. Keratocystic odontogenic tumour: Reclassification of the odontogenic keratocyst from cyst to tumour. J Can Dent Assoc 74:165–165h.

Moan J, Dahlback A, Henriksen T, Magnus K. 1989. Biological amplification factor for sun-light-induced nonmelanoma skin cancer at high latitudes. Cancer Res 49:5207–5212.

Morgan TA, Burton CC, Qian F. 2005. A retrospective review of treatment of the odontogenic keratocyst. J Oral Maxillofac Surg 63:635–639.

Nagao K, Togawa N, Fujii K, Uchikawa H, Kohno Y, Yamada M, Miyashita T. 2005. Detecting tissue-specific alternative splicing and disease-associated aberrant splicing of the *PTCH* gene with exon junction microarrays. Hum Mol Genet 14:3379–3388.

Nagao K, Fujii K, Saito K, Sugita K, Endo M, Motojima T, Hatsuse H, Miyashita T. 2011. Entire *PTCH1* deletion is a common event in point mutation-negative cases with nevoid basal cell carcinoma syndrome in Japan. Clin Genet 79:196–198.

Nakayama M, Tabuchi K, Nakamura Y, Hara A. 2011. Basal cell carcinoma of the head and neck. J Skin Cancer 2011:496910.

Richmond-Sinclair NM, Pandeya N, Ware RS, Neale RE, Williams GM, van der Pols JC, Green AC. 2009. Incidence of basal cell carcinoma multiplicity and detailed anatomic distribution: Longitudinal study of an Australian population. J Invest Dermatol 129:323–328.

Rubin AI, Chen EH, Ratner D. 2005. Basal-cell carcinoma. N Engl J Med 353:2262–2269.

Sasaki R, Miyashita T, Matsumoto N, Fujii K, Saito K, Ando T. 2010. Multiple keratocystic odontogenic tumors associated with nevoid basal cell carcinoma syndrome having distinct *PTCH1* mutations: A case report. Oral Surg Oral Med Oral Pathol Oral Radiol Endod 110:e41–e46.

Shanley S, Ratcliffe J, Hockey A, Haan E, Oley C, Ravine D, Martin N, Wicking C, Chenevix-Trench G. 1994. Nevoid basal cell carcinoma syndrome: Review of 118 affected individuals. Am J Med Genet 50: 282–290.

Smucker PS, Smith JL. 2006. Multifocal desmoplastic medulloblastoma in an African-American child with nevoid basal cell carcinoma (Gorlin) syndrome. Case report. J Neurosurg 105:315–320.

Unden AB, Holmberg E, Lundh-Rozell B, Ståhle-Bäckdahl M, Zaphiropoulos PG, Toftgård R, Vorechovsky I. 1996. Mutations in the human homologue of Drosophila patched (PTCH) in basal cell carcinomas and the Gorlin syndrome: Different in vivo mechanisms of PTCH inactivation. Cancer Res 56:4562–4565.

Wicking C, Shanley S, Smyth I, Gillies S, Negus K, Graham S, Suthers G, Haites N, Edwards M, Wainwright B, Chenevix-Trench G. 1997. Most germ-line mutations in the nevoid basal cell carcinoma syndrome lead to a premature termination of the PATCHED protein, and no genotype–phenotype correlations are evident. Am J Hum Genet 60:21–26.

Splicing Aberration in Naevoid Basal Cell Carcinoma Syndrome

Yosuke Ishitsuka[1], Junichi Furuta[1], Toshiyuki Miyashita[2] and Fujio Otsuka[1]

[1]Department of Dermatology, Graduate School of Comprehensive Human Sciences, University of Tsukuba, 1-1-1, Ten-nodai, Tsukuba, Ibaraki and [2]Department of Molecular Genetics, Kitasato University, School of Medicine, Kanagawa, Japan. E-mail: c0930412@md.tsukuba.ac.jp

Accepted November 30, 2011.

Pre-RNA splicing is a transcriptional process whereby introns are removed from a primary transcript and exons are joined to generate a mature protein-coding mRNA transcript. The reaction is initiated by transcripts binding to spliceosomal protein complexes that recognize splice site signals at exon/intron boundaries (1). The flexibility of splice sites in individual genes facilitates complex gene regulation and protein diversity by alternative splicing (2). Alterations in splice site selection, can be affected by gene mutations and may cause splicing modifications. A new "cryptic" splice site can replace the original because of a change in spliceosome affinity (3) and has pathogenic consequences if there is an amino acid change or a protein truncation.

Naevoid basal cell carcinoma syndrome (NBCCS) is caused by germline mutations in the *patched protein homolog 1* (*PTCH1*) (4, 5). NBCCS is characterized by a predisposition to neoplasms and a range of developmental anomalies (6), including multiple basal cell carcinomas (BCCs), odontogenic keratocysts, palmoplantar pits and bifid ribs. *PTCH1* is located on chromosome 9q22.3 (7), where it encodes a receptor protein for the hedgehog signalling pathway (8) that plays an important role in developmental processes such as cell polarity and pattern formation (9).

This study tested the benefits of additional mRNA analysis in a NBCCS patient in whom a mutation was identified by genomic sequencing as splicing aberration.

CASE REPORT

A 58-year-old Japanese man with a history of congenital hydrocephaly and previous extirpation of a jaw cyst during his teenage years noticed black nodules on his face and thighs, which were excised after they were diagnosed as BCCs. He had no family history of NBCCS, but his face presented the characteristic manifestation of hypertelorism, and multiple pits were observed on his palms and soles. Pantomography identified multiple odontogenic keratocysts in his mandible, while a skull MRI indicated communicating hydrocephalus. The patient was diagnosed with NBCCS after satisfying 3 major diagnostic criteria (10), namely, the presence of multiple BCCs, palmoplantar pits and odontogenic keratocysts. Mutational analysis (see http://www.medicaljournals.se/acta/content/?doi=10.2340/00015555-1332) for details including references to (11) and (12).

Prior to commencing this study, written informed consent was obtained from the patient and permission was obtained from the ethical committee of Tsukuba University Hospital.

A mutation analysis of *PTCH1* was made to investigate the cause of the patient's symptoms. We extracted genomic DNA from the patient's peripheral blood and performed genomic sequencing, which revealed a mutation site where the 584th guanine (G) was replaced by adenine (A) (c.584G>A) on exon 3 (as per GenBank entry NM_000264) (Fig. 1A). This mutation was identified in a previous study (11, 13), but this point mutation suggested a missense mutation whereby the 195th amino acid arginine was replaced by lysine (p.R195K). However, the mutation could affect splicing because the mutation was located at the 3′ end of exon 3. Therefore, we established an immortalized cell line from the patient's lymphoblastoid cells to obtain mRNA, which was then subjected to RT-PCR. Electrophoresis of the product revealed an additional large band (Fig. 1C). Sequencing of the additional product indicated the activation of a cryptic 5′ splice site in intron 3 and the insertion of a 37-bp intronic sequence, which included a termination signal, resulting in premature termination of translation (Fig. 1E). This demonstrated the presence of a splicing aberration and suggested the formation of a truncated PTCH1 protein as a result of the c.584G>A mutation. Thus, we concluded that this NBCCS case was attributable to a splicing aberration.

DISCUSSION

The *PTCH1* mutation identified in the present case was located at an exon/intron boundary, where it could disrupt the splicing signal, so it was reasonable to predict a splicing aberration. However, aberrant splicing can also be caused by silent mutations in which single base substitutions do not change specific amino acids. Indeed, a mutation in *LAMB3* of a junctional epidermolysis bullosa patient initially appeared to be a silent mutation, but it actually resulted in the aberrant splicing of a cryptic splice site (14). A comparative study of mRNA and genomic DNA in neurofibromatosis patients showed that 50% of the patients had mutations resulting in splicing aberration, which was confirmed by mRNA analysis, although 37% of the patients had splice site mutations that were identified without cDNA sequencing (15). Therefore, these previous studies and the present case clearly illustrate the significance of additional cDNA sequencing after the identification of a genomic mutation. An aggregate analysis of NBCCS patients with genomic mutations revealed that two out of 28 patients (7.1%) had splice site mutations (16). However, our study indicates that the actual incidence of splicing aberrations among NBCCS patients might be higher.

In addition, we extracted a sample from the patient's peripheral blood, because peripheral blood monocytes express the PTCH1 protein. Moreover, analysis of *PTCH1* mRNA and genomic DNA can be performed using samples obtained from patients' peripheral blood. Although splicing patterns may differ depending on the tissues examined, our method was less invasive and more appropriate for multiple subjects with NBCCS compared with a procedure that requires disease tissue.

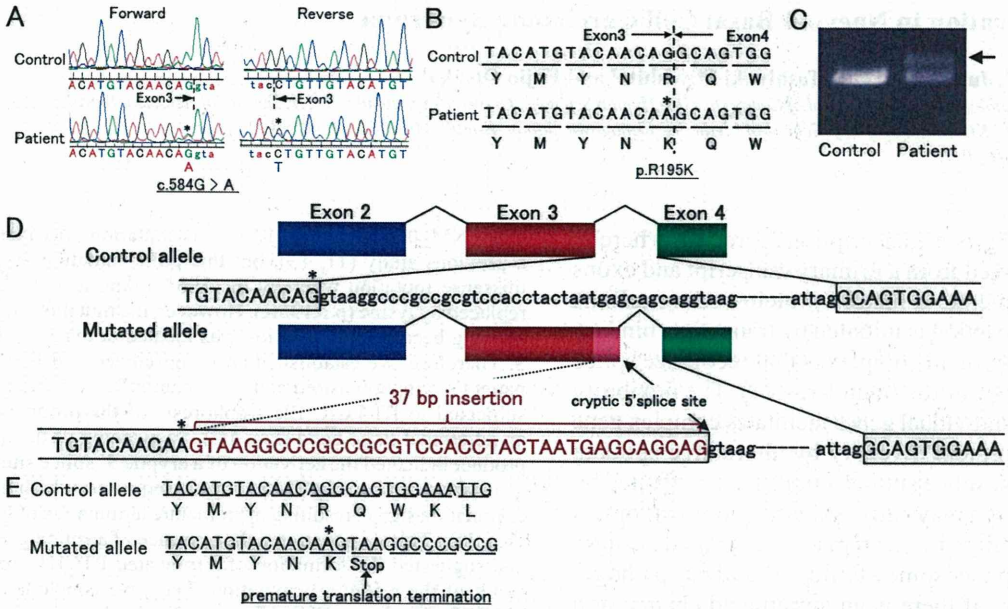

Fig. 1. The mutation identified in the patient and its effect on the splicing event. In parts (A) and (D), the exonic sequence is denoted by uppercase letters, while the intronic sequence is denoted by lowercase letters. A sample from a healthy donor was used as a control. (A) Genomic sequence of *PTCH1*. The 584th guanine (G) was replaced by adenine (A) in the patient's DNA. Note the double peaks at the last base in exon 3 (*green and red*). (B) The patient's amino acid sequence predicted from the genomic mutation c.584G>A. The 195th amino acid, arginine (R), would be substituted with lysine (K). (C) Electrophoresis of cDNA obtained from the mRNA, which was extracted from the patient's Epstein-Barr virus (EBV)-immortalized lymphoblastoid cells. Note the additional large band in the patient's lane (*arrow*). (D) Schematic representation of the splicing aberration found in the patient. A 37-bp sequence (*red letters*) was inserted following a mutation located in the 3′ end of exon 3 (*asterisks*). Because of the base substitution at the 3′ end of exon 3 (G → A), a cryptic 5′ splice site was produced in intron 3 (*double-headed arrow*), rather than the original site at the intron/exon border. This resulted in a splicing aberration on activation. (E) Results of cDNA sequencing. In addition to the amino acid alteration, a frameshift mutation due to the splicing aberration caused a termination signal (TAA) that resulted in the truncation of the PTCH1 protein.

REFERENCES

1. House AE, Lynch KW. Regulation of alternative splicing: more than just the ABCs. J Biol Chem 2008; 283: 1217–1221.
2. Smith CW, Valcarcel J. Alternative pre-mRNA splicing: the logic of combinatorial control. Trends Biochem Sci 2000; 25: 381–388.
3. Wessagowit V, Nalla VK, Rogan PK, McGrath JA. Normal and abnormal mechanisms of gene splicing and relevance to inherited skin diseases. J Dermatol Sci 2005; 40: 73–84.
4. Johnson RL, Rothman AL, Xie J, Goodrich LV, Bare JW, Bonifas JM, et al. Human homolog of patched, a candidate gene for the basal cell nevus syndrome. Science 1996; 272: 1668–1671.
5. Hahn H, Wicking C, Zaphiropoulous PG, Gailani MR, Shanley S, Chidambaram A, et al. Mutations of the human homolog of Drosophila patched in the nevoid basal cell carcinoma syndrome. Cell 1996; 85: 841–851.
6. Gorlin RJ. Nevoid basal-cell carcinoma syndrome. Medicine (Baltimore) 1987; 66: 98–113.
7. Hahn H, Christiansen J, Wicking C, Zaphiropoulos PG, Chidambaram A, Gerrard B, et al. A mammalian patched homolog is expressed in target tissues of sonic hedgehog and maps to a region associated with developmental abnormalities. J Biol Chem 1996; 271: 12125–12128.
8. Stone DM, Hynes M, Armanini M, Swanson TA, Gu Q, Johnson RL, et al. The tumour-suppressor gene patched encodes a candidate receptor for Sonic hedgehog. Nature 1996; 384: 129–134.
9. Lum L, Beachy PA. The Hedgehog response network: sensors, switches, and routers. Science 2004; 304: 1755–9175.
10. Kimonis VE, Goldstein AM, Pastakia B, Yang ML, Kase R, DiGiovanna JJ, et al. Clinical manifestations in 105 persons with nevoid basal cell carcinoma syndrome. Am J Med Genet 1997; 69: 299–308.
11. Fujii K, Kohno Y, Sugita K, Nakamura M, Moroi Y, Urabe K, et al. Mutations in the human homologue of Drosophila patched in Japanese nevoid basal cell carcinoma syndrome patients. Hum Mutat 2003; 21: 451–452.
12. Coyaud E, Struski S, Prade N, Familiades J, Eichner R, Quelen C, et al. Wide diversity of PAX5 alterations in B-ALL: a Groupe Francophone de Cytogenetique Hematologique study. Blood 2010; 115: 3089–3097.
13. Nagao K, Togawa N, Fujii K, Uchikawa H, Kohno Y, Yamada M, et al. Detecting tissue-specific alternative splicing and disease-associated aberrant splicing of the PTCH gene with exon junction microarrays. Hum Mol Genet 2005; 14: 3379–3388.
14. Buchroithner B, Klausegger A, Ebschner U, Anton-Lamprecht I, Pohla-Gubo G, Lanschuetzer CM, et al. Analysis of the LAMB3 gene in a junctional epidermolysis bullosa patient reveals exonic splicing and allele-specific nonsense-mediated mRNA decay. Lab Invest 2004; 84: 1279–1288.
15. Ars E, Serra E, Garcia J, Kruyer H, Gaona A, Lazaro C, et al. Mutations affecting mRNA splicing are the most common molecular defects in patients with neurofibromatosis type 1. Hum Mol Genet 2000; 9: 237–247.
16. Wicking C, Shanley S, Smyth I, Gillies S, Negus K, Graham S, et al. Most germ-line mutations in the nevoid basal cell carcinoma syndrome lead to a premature termination of the PATCHED protein, and no genotype-phenotype correlations are evident. Am J Hum Genet 1997; 60: 21–26.

Mutational analysis: DNA was extracted using a QIAamp DNA Blood Mini Kit (Qiagen, MD, USA). Genomic DNA samples were amplified using primers for each exon, as previously described (11). Amplified products were gel-purified using a QIAEX II Gel Extraction Kit (Qiagen). Sequencing reactions were performed using a GenomeLab DTCS Quick Start Kit (Beckman Coulter, CA, USA) with a cycle sequencing protocol, while sequencing reactions were separated on a CEQ 8000 Genetic Analysis System (Beckman Coulter). Splicing aberrations were tested using an immortalized cell line that was established from the patient by infecting with Epstein-Barr virus (EBV) (12) obtained from B95-8 cells. Total RNA was extracted from the EBV-immortalized lymphoblastoid cell line using a QIAamp RNA Blood Mini Kit (Qiagen) and subjected to reverse transcription (RT)-PCR using a Long-Range 2-Step RT-PCR Kit (Qiagen) with oligo dT. The forward and reverse primers for exons 2 and 6 were 5′-GCTGAGAGCGAAGTTTCAGA-3′ and 5′-CCAGGAATTCCAAAGGGTCGAAG-3′, respectively.

Inhibition of cell viability by human IFN-β is mediated by microRNA-431

TAKESHI TANAKA[1], SHIGERU SUGAYA[1], KAZUKO KITA[1], MAKOTO ARAI[2], TATSUO KANDA[2], KATSUNORI FUJII[3], FUMIO IMAZEKI[2], KATSUO SUGITA[4], OSAMU YOKOSUKA[2] and NOBUO SUZUKI[1]

Departments of [1]Environmental Biochemistry, [2]Medicine and Clinical Oncology, [3]Pediatrics, Graduate School of Medicine, Chiba University, 1-8-1 Inohana, Chiba 260-8670; [4]Faculty of Education, Chiba University, 1-33 Yayoichou, Chiba 263-8522, Japan

Received September 15, 2011; Accepted November 17, 2011

DOI: 10.3892/ijo.2012.1345

Abstract. MicroRNAs (miRNAs) are small non-coding RNAs that inhibit gene expression by cleaving or hindering the translation of target mRNAs. We used microarray-based comparative transcriptome analysis to identify changes in miRNA expression and function between a human cell line, RSa, which is highly sensitive to HuIFN-β-mediated inhibition of cell viability, and its variant, the F-IF^r cell line, which is relatively resistant to the cytokine. miR-431 expression was significantly higher in RSa cells compared with F-IF^r cells. The addition of HuIFN-β to RSa cultures reduced cell viability, down-regulated expression of *IGF1R* and *IRS2* (putative miR-431 target genes), and inhibited the PI3K-Akt and MAPK pathways. The survival of F-IF^r cells was not reduced by HuIFN-β, but transient transfection with miR-431 precursors significantly decreased viability and concomitantly down-regulated *IGF1R* and *IRS2* expression. In addition, the MAPK pathway, but not the PI3K-Akt pathway, was suppressed in F-IF^r cells. Based on these results, we propose that, in RSa cells, HuIFN-β-induced miR-431 expression may down-regulate *IGF1R* and *IRS2* expression, and consequently inhibit cell proliferation by suppressing the MAPK pathway.

Introduction

MicroRNAs (miRNAs) are small non-coding RNAs that regulate gene expression by base pairing specifically with nucleotides in the 3' untranslated regions of target mRNAs or by directing mRNA degradation (1). MiRNAs play important roles in cell proliferation, apoptosis, and differentiation (2,3). In particular, miRNAs that regulate cell proliferation have been implicated in various cancers. Numerous studies have revealed differences in the expression of various miRNAs between tumors and normal tissues (4), suggesting that miRNAs can function as either tumor suppressors or oncogenes in human cancers. In addition, there are a number of reports demonstrating that certain miRNAs participate in the activity of various anti-cancer drugs. For example, the combination of miR-145 and 5-fluorouracil (5-FU) has an anti-tumor effect on breast cancer (5). In a non-small cell lung cancer cell line (A549), cisplatin sensitivity was increased by up-regulating miR-451 expression (6). In contrast, miR-21 induced resistance to the anti-cancer effects of IFN-α/5-FU combination therapy in hepatocellular carcinoma cells (7). Human interferons (HuIFNs) are a family of cytokines that have various biological functions, including anti-viral and anti-tumor activity (8). They also regulate basic cellular functions including growth, differentiation, and immune reactivity (9-11). HuIFNs induce a cascade of events leading to an increase in the expression of various genes, including those responsible for the biological effects of IFNs (9-13). HuIFNs are divided into type I, II, and III subtypes, based in part on the differential use of unique receptors through which they mediate their biological effects. HuIFN-α and -β are type I IFNs. HuIFN-β has proven useful as an anti-neoplastic drug, although the role of miRNAs in this function is not clear. In this study, we focused on the miRNAs that were induced by HuIFN-β using the HuIFN-β-sensitive cell line, RSa, and its resistant variant, the F-IF^r cell line. Our aim was to identify miRNAs that are up-regulated by HuIFN-β and are responsible for suppressing cell proliferation in human cells.

Materials and methods

Cell lines and culture conditions. RSa cells were established from human embryo-derived fibroblasts by double infection with Simian virus 40 and Rous sarcoma virus. These cells are highly sensitive to the ability of HuIFN-β to inhibit cell viability. The F-IF^r line is a variant with increased resistance to HuIFN-β. Both cell lines were cultured in Eagle's minimal essential medium (EMEM; Nissui, Tokyo, Japan) containing 10% calf serum (CS; Invitrogen, Carlsbad, CA, USA) at 37°C in a humidified atmosphere containing 5% CO_2.

RNA extraction. Total RNA was extracted using TRIzol reagent (Invitrogen) according to the manufacturer's instructions.

Correspondence to: Dr Takeshi Tanaka or Dr Nobuo Suzuki, Department of Environmental Biochemistry, Graduate School of Medicine, Chiba University, 1-8-1 Inohana, Chiba 260-8670, Japan
E-mail: take64@faculty.chiba-u.jp
E-mail: nobuo@faculty.chiba-u.jp

Key words: microRNA, human IFN-β, IGF signaling pathway, cell viability, cancer therapy

Microarray analysis. We analyzed miRNA expression using Genopal®-MICH chips (Mitsubishi Rayon, Yokohama, Japan), equipped with 188 oligonucleotide DNA probes in hollow plastic fibers for detection of human miRNAs. Hybridization signals were analyzed using a DNA chip analyzer according to the manufacturer's instructions.

Estimation of miRNA expression levels. Quantitative RT-PCR for three miRNAs (miR-193b, miR-381, and miR-431) was carried out using the TaqMan MicroRNA Assay (Applied Biosystems, Foster City, CA, USA). Total RNA (30 ng) from RSa and F-IF^r cells were reverse-transcribed using the TaqMan Reverse Transcription kit (Applied Biosystems) according to the manufacturer's protocol. For normalization, each miRNA was amplified on the same plate with the reference miRNA, RNU6B, and we calculated changes in expression levels relative to this standard.

HuIFN-β and PI3K inhibitor LY294002 treatment. Recombinant human IFN-β was obtained from PeproTech (Rocky Hill, NJ, USA). PI3K inhibitor LY294002 was obtained from Cosmo Bio (Tokyo, Japan). Briefly, logarithmically growing RSa and F-IF^r cells were plated at a density of $5x10^5$ cells/35-mm culture dish, and after 24 h, the medium was replaced with fresh EMEM or the same medium containing HuIFN-β (at either 100 or 500 IU/ml) or PI3K inhibitor LY294002 (75 μM).

Measurement of cell viability. Cell viability was measured from the average of 6 MTS assays per sample, quantified by absorbance at 490 nm in a microplate colorimeter using the CellTiter 96 AQueous One Solution Reagent (Promega, Madison, WI, USA) according to the manufacturer's instructions, for each time point.

Transfection of miRNA molecules. MiRNA precursors that mimic miR-381 or miR-431, a control non-specific miRNA (Pre-miR Negative Control), and anti-miRNA molecules were obtained from Ambion (Austin, TX, USA). Using siPORT NeoFX (Ambion), miRNA precursors were transfected into F-IF^r cells and anti-miRNA molecules into RSa cells, according to the manufacturer's protocol. For siRNA transfection, cells (plated to reach 80% confluence after 12 or 24 h) were treated with siRNAs complementary to each target gene or a control using siPORT NeoFX. Predicted target genes for miRNA were identified using TargetScan (http://www.targetscan.org).

Western blotting. Cells grown to 80% confluence were treated with HuIFN-β, pre-miR-431 or anti-miR-431. After treatment, cells were washed three times with ice-cold PBS. Equal amounts of protein were separated by SDS-PAGE and transferred to polyvinylidene fluoride membranes (ATTO, Tokyo, Japan). Membranes were blocked in 5% non-fat dried milk in PBST and incubated with primary antibody. The following antibodies were used: IGF-1Rα, IGF-1Rβ, IRS2, and total Akt1/2/3 from Santa Cruz Biotechnology, Santa Cruz, CA, USA; p-Akt (phospho-Akt, Thr^{308}), p-Akt (phospho-Akt, Ser^{473}), p44/42 MAPK (Erk1/2), and phosphor-p44/42 MAPK (Erk1/2), from Cell Signaling Technology (Danvers, MA, USA). GAPDH (Sigma, St. Louis, MO, USA) was used as an internal control. Secondary antibodies were conjugated to horseradish peroxidase and immunoreactive proteins were detected using the ECL-plus system (Amersham, Piscataway, NJ, USA).

Estimation of miRNA target gene expression. Total RNA (30 ng) from F-IF^r cells was reverse-transcribed using Super Script III First-Strand Synthesis SuperMix (Invitrogen) according to the manufacturer's protocol. Steady-state expression levels of *IGF1R* and *IRS2* mRNAs were evaluated by quantitative RT-PCR using Fast SYBR Green Master Mix and the following oligonucleotide primers and annealing temperatures: *IGF1R*, 5'-CATCGACATCCGCAACGA-3' (forward) and 5'-CCCTCGATCACCGTGCA-3' (reverse) at 50°C; *IRS2*, 5'-GT ACCTGATCGCCCTCTAC-3' (forward) and 5'-AGGCACA GACGGTACAC-3' (reverse) at 50°C. Expression of each gene was normalized to a GAPDH control: 5'-ACCCACTCCTCCA CCTTTG-3' (forward) and 5'-CTCTTGTGCTCTTGCTGG G-3' (reverse).

Results

Comparison of miRNA expression levels between RSa and F-IF^r cells. MiRNA expression levels in RSa cells were compared to those in F-IF^r cells by microarray analysis. The levels of miR-193b, miR-381, and miR-431 were significantly higher in RSa cells, being over 5-fold greater than in F-IF^r cells (data not shown). Quantitative RT-PCR analysis of the three miRNAs revealed a significantly higher expression of miR-381 and miR-431 (3.56- and 3.81-fold greater, respectively) in RSa cells relative to F-IF^r cells.

Effect of HuIFN-β on cell viability and miR-431 expression. When HuIFN-β was added to culture medium at a concentration 500 IU/ml, a significant suppression of RSa cell viability was observed 24 h later (Fig. 1A). In contrast, F-IF^r cell viability was not significantly suppressed by HuIFN-β, at any dose up to 500 IU/ml, nor by any duration up to 24 h (Fig. 1B). HuIFN-β (500 IU/ml) induced a significant increase in miR-431 expression in RSa cells relative to F-IF^r cells 24 h following addition, but it did not affect miR-381 expression (Fig. 1C).

Examination of the role of miR-431 on cell viability. In order to examine whether increased expression of miR-431 results in reduced cell viability, F-IF^r cells were transiently transfected with miR-431, this resulted in a significant suppression of cell viability 24 h later (Fig. 2A). No significant effect on viability was observed following transfection with miR-381 (Fig. 2A). When RSa cells were treated with both HuIFN-β and anti-miR-431, cell proliferation was not suppressed at 24 h (Fig. 2B).

Search for miR-431 target genes. Predicted target genes for miR-431 were identified with TargetScan (Table I). Among these genes, we focused on the cell viability-related genes, *IGF1R* (insulin-like growth factor 1 receptor) and *IRS2* (insulin receptor substrate 2). Schematic representation of *IGF1R* and *IRS2* mRNAs, showing the predicted miR-431 binding sites located in their 3' UTR, are given in Fig. 3A. To determine the effects of reducing *IGF1R* or *IRS2* mRNA levels on cell viability, we assessed the viability of F-IF^r cells treated with gene-specific siRNAs or a non-targeting control siRNA. Treatment with the

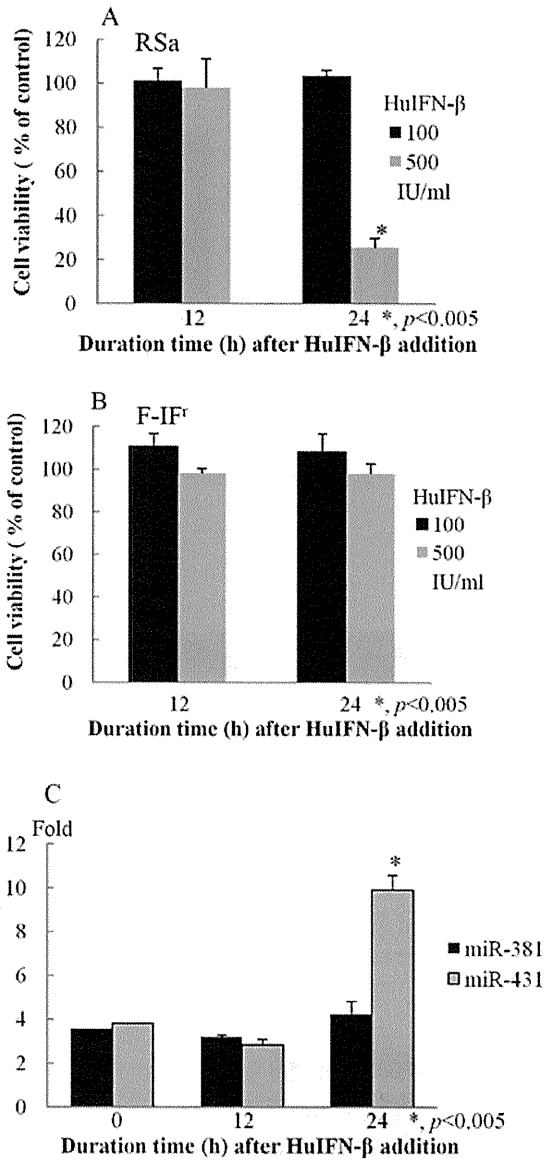

Figure 1. Effect of HuIFN-β treatment on cell viability and expression levels of miRNAs. (A and B), HuIFN-β was added to the culture medium of RSa and F-IFr cells, at 100 IU/ml (black) or 500 IU/ml (grey) (*p<0.005, t-test). (C), Quantitative RT-PCR was performed to examine the effects of a 24-h HuIFN-β (500 IU/ml) treatment on miR-381 (black) and miR-431 (grey) expression in RSa cells relative to F-IFr cells. MiRNA expression is presented as a fold difference with respect to F-IFr cells, with the value for F-IFr cells set at a fold change of 1. Results are presented as the means ± SD *p<0.005.

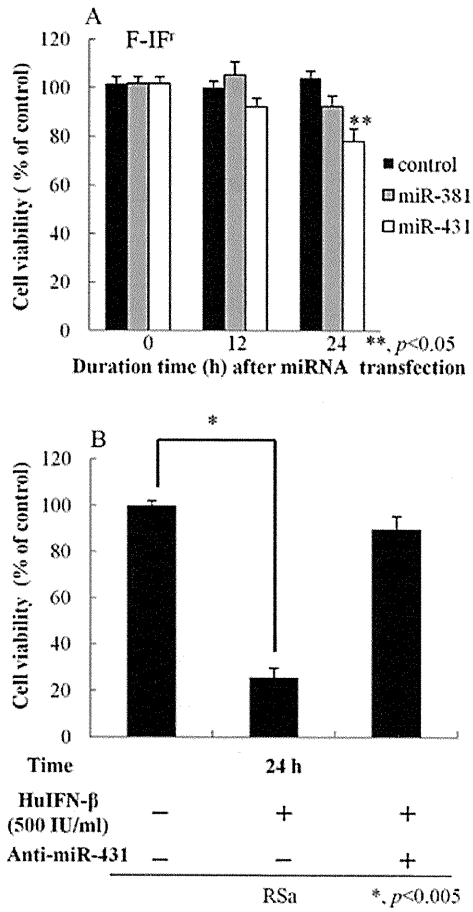

Figure 2. Effects of miRNA transient transfection or HuIFN-β treatment with or without anti-miR-431 addition on cell viability. (A), Transient transfection with miR-381 (grey) or miR-431 (white) in F-IFr cells (**p<0.05, t-test). (B), Changes in cell viability in RSa cells treated with HuIFN-β with or without anti-miR-431. Results are presented as the means ± SD. *p<0.005, **p<0.05.

siRNAs led to a significant suppression of cell viability relative to control cells (Fig. 3B).

Examination of IGF1R signaling pathways. When RSa cells were treated with HuIFN-β (500 IU/ml), a reduction in protein levels of IGF1Rα/β and IRS2 was consistently observed after 24 h (Fig. 4A). A similar reduction was also detected in F-IFr cells transfected with miR-431 precursors (Fig. 4B). However,

Table I. Predicted miR-431 targets involved in cell viability.[a]

Gene symbol	Gene name	Conserved sites				Poorly conserved sites				Total cont. score
		Total	8-mer	7-mer-m8	7-mer-1A	Total	8-mer	7-mer-m8	7-mer-1A	
IGF1R	Insulin-like growth factor 1 receptor	1	1	0	0	0	0	0	0	-0.17
IRS2	Insulin receptor substrate 2	1	1	0	0	0	0	0	0	-0.37

[a]Targets for miR-431 were predicted using TargetScanHuman 5.2. Total cont. score, total context score.

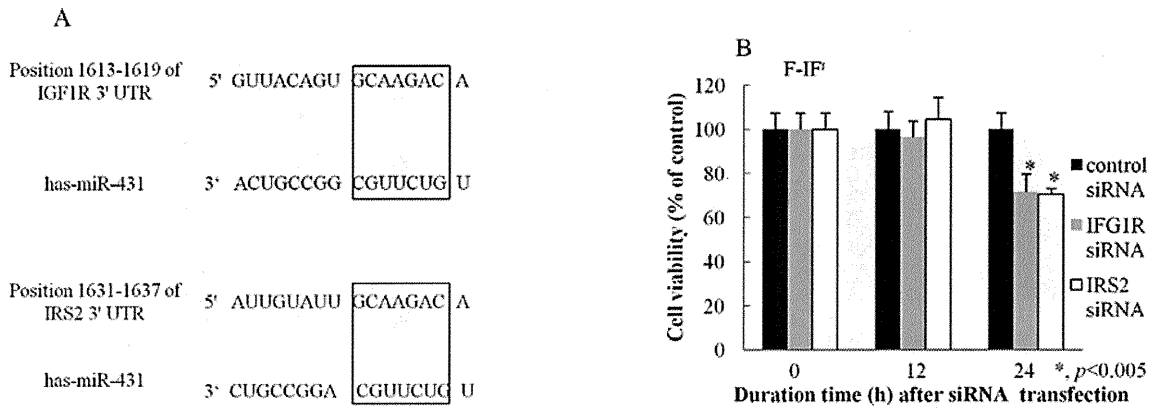

Figure 3. Cell viability after transient transfection with siRNA (*IGF1R* or *IRS2*) in F-IF^r cells. (A), Sites of miR-431 seed matching in the *IGF1R* and *IRS2* 3' UTRs. (B), Transfection with control siRNA (black) or *IGF1R* (grey) or *IRS2* (white) siRNA in F-IF^r cells, respectively. A significant suppression of cell viability was observed in F-IF^r cells at 24 h relative to the control. Results are presented as means ± SD. *p<0.005.

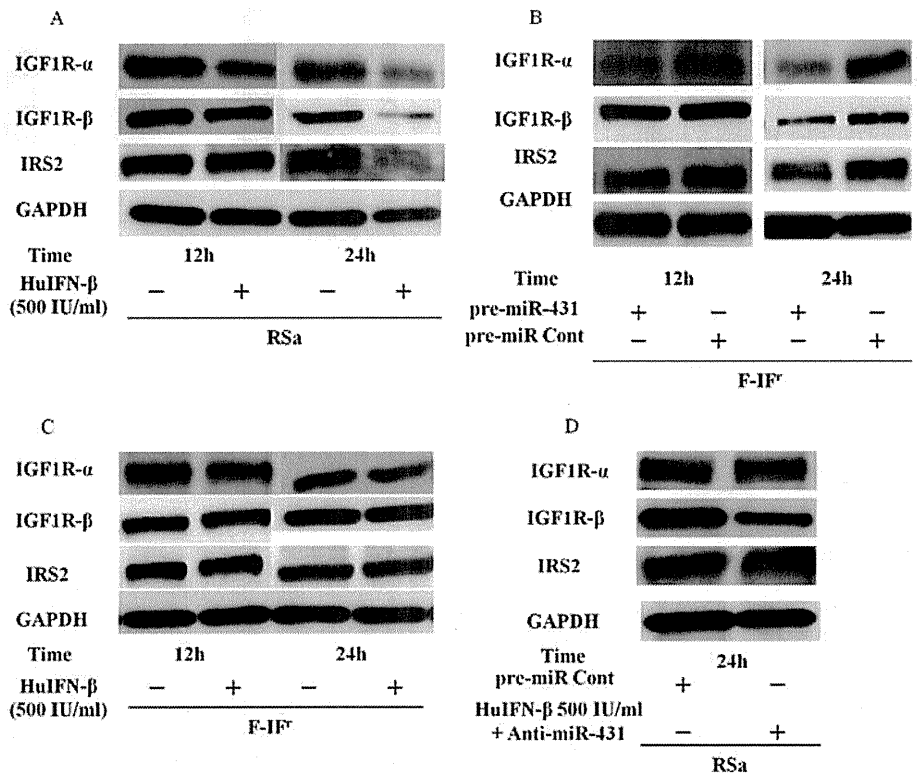

Figure 4. Effects of HuIFN-β and miR-431 on *IGF1R* and *IRS2* expression. (A and C), Immunoblots of IGF1R (α/β) and IRS2 proteins in RSa and F-IF^r cells with or without HuIFN-β (500 IU/ml) treatment. (B), The levels of IGF1R (α/β) and IRS2 in F-IF^r cells transfected with pre-miR-431 and pre-miR negative control precursors for 12 or 24 h. (D), Expression levels of IGF1R and IRS2 in RSa cells treated with HuIFN-β (500 IU/ml) and anti-miR-431 for 24 h. GAPDH was used as a loading control.

no apparent change in protein levels was observed when F-IF^r cells were treated with HuIFN-β (Fig. 4C). HuIFN-β (500 IU/ml) and anti-miR-431 treatment resulted in a significant increase in the expression of IGF1R and IRS2 in RSa cells (Fig. 4D).

Since IGF1R is a major player in the PI3K-Akt and MAPK signaling pathways, we investigated the effects of miR-431-mediated *IGF1R* down-regulation on PI3K-Akt and MAPK phosphorylation. In RSa cells, protein levels of total Akt, p-Akt Thr^{308}, p-Akt Ser^{473}, total Erk1/2, and p-Erk1/2 were reduced after 24 h of HuIFN-β (500 IU/ml) treatment (Fig. 5A). In contrast, the levels of these proteins were not changed in F-IF^r cells (Fig. 5B). When F-IF^r cells were transfected with miR-431 precursors, reductions in the levels of total Erk1/2 and p-Erk1/2 were observed after 24 h of transfection, while the levels of total Akt, p-Akt Thr^{308}, and p-Akt Ser^{473} were

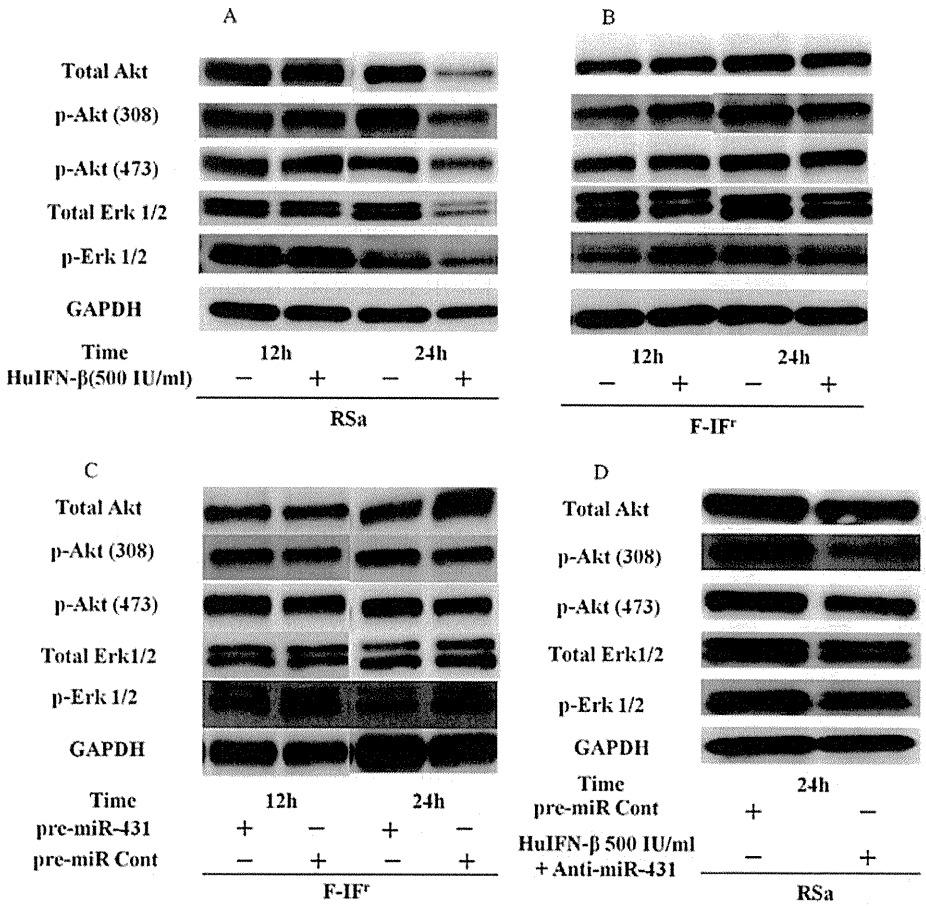

Figure 5. Inhibition of the PI3K-Akt and MAPK pathways targeted by HuIFN-β and miR-431. (A and B), Immunoblots of total Akt, p-Akt (Ser^{473}, Thr^{308}), total Erk1/2, and p-Erk1/2 in RSa and F-IF^r cells with or without treatment with HuIFN-β (500 IU/ml) for 12 or 24 h. (C), The levels of total Akt, p-Akt (Ser^{473}, Thr^{308}), total Erk1/2, and p-Erk1/2 in F-IF^r cells which were transfected with pre-miR-431 or pre-miR control precursors for 12 or 24 h. (D), The levels of total Akt, p-Akt (Ser^{473}, Thr^{308}), total Erk1/2, and p-Erk1/2 in RSa cells which were treated with HuIFN-β (500 IU/ml) and anti-miR-431 for 24 h. GAPDH was used as a loading control.

not significantly altered (Fig. 5C). Knockdown of miR-431 by anti-miR-431 and simultaneous treatment with HuIFN-β (500 IU/ml) removed the suppression of total Akt, p-Akt Thr^{308}, p-Akt Ser^{473}, total Erk1/2, and p-Erk1/2 expression in RSa cells (Fig. 5D).

Suppression of miR-431 target genes. Transient transfection with miR-431 precursors significantly suppressed *IGF1R* and *IRS2* expression in F-IF^r cells after 24 h relative to control-transfected cells (Fig. 6A). Treating RSa cells with HuIFN-β (500 IU/ml) also significantly diminished *IGF1R* and *IRS2* expression after 24 h relative to control cells (Fig. 6B). However, when RSa cells were treated with both HuIFN-β (500 IU/ml) and anti-miR-431, *IGF1R* and *IRS2* expression were not significantly affected (Fig. 6B).

Effect of PI3K inhibitor on cell viability. F-IF^r cells were transfected with miR-431 precursors and/or the PI3K inhibitor LY294002. Proliferation was reduced by approximately 20% when cells were transfected with miR-431 precursors. However, it was suppressed approximately 30% when cells were transfected with miR-431 precursors and treated with LY294002 at the same time (Fig. 7).

Discussion

There are numerous reports of the involvement of miRNAs in regulating cell proliferation in a multitude of cancer cell lines (4). We focused on a few miRNAs whose expression levels were altered by the addition of HuIFN-β in a non-cancer HuIFN-β sensitive cell line, RSa, and its variant HuIFN-β resistant cell line, F-IF^r.

Based on microarray analysis, we focused on three miRNAs (miR-193b, miR-381, and miR-431) whose expression levels were up-regulated more than 5-fold in RSa cells relative to F-IF^r cells. Among these, miR-381 and miR-431 were also up-regulated according to quantitative RT-PCR. In addition, HuIFN-β treatment increased miR-431 expression and reduced cell viability in RSa cells (Fig. 1A and C). In contrast, transfection of miR-431 precursors into F-IF^r cells significantly reduced cell viability (Fig. 2A). These results suggest that miR-431 plays a role in regulating cell viability.

We then sought to determine whether miRNA-regulated signaling pathways modulated cell viability. Previous reports revealed that some signaling pathways that affect cell viability are regulated by miRNAs (14-19). We decided to focus on one of these - the IGF signaling pathway. The factors that activate IGF

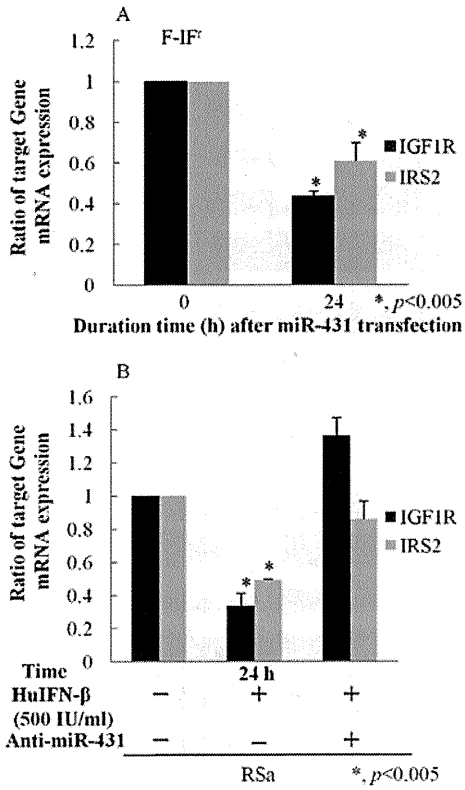

Figure 6. *IGF1R* and *IRS2* mRNA expression. (A), Quantitative RT-PCR was performed to examine the effects of miR-431 on IGF1R (black) and IRS2 (grey) mRNA levels in F-IF^r cells that were transfected with pre-miR-431 precursors or the pre-miR control. mRNA expression levels are presented as a fold difference with respect to F-IF^r cells transfected with the pre-miR control, which was set at a fold change of 1. (B), IGF1R (black) and IRS2 (grey) mRNA levels were analyzed by quantitative RT-PCR after 24 h following HuIFN-β addition in combination with anti-miR-431 treatment. mRNA expression levels are presented as a fold difference with respect to control RSa cells [HuIFN-β(-), anti-miR-431(-)] which was set at a fold change of 1. Results are presented as the means ± SD. *p<0.005.

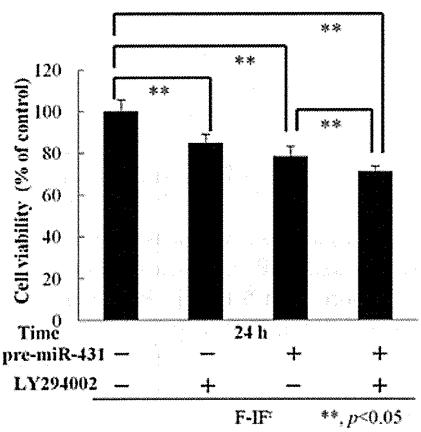

Figure 7. Effects of pre-miR-431 and the PI3K inhibitor on cell viability. F-IF^r cells were transfected with pre-miR-431 precursors and/or treated with the PI3K inhibitor LY294002. Results are presented as means ± SD. **p<0.05.

signaling pathways and promote cell proliferation in cancers have been investigated by others (20). For numerous cancers, the activation of IGF signaling pathways contributes to cell proliferation. Therefore, the suppression of this pathway should inhibit cancer cell proliferation. In tongue squamous cell carcinoma, miR-7 levels are reduced, but the ectopic expression of miR-7 significantly down-regulates IGF1R expression, at both the mRNA and protein levels (21). Thus, a miRNA can suppress a cell growth-signaling pathway.

In the present study, we examined the miR-431 target genes that are suspected of suppressing cell viability, and focused on *IGF1R* and *IRS2*, which are functional targets of miR-431. IGF1R is a receptor tyrosine kinase that consists of heterotetramers ($\alpha_2\beta_2$) held together by disulfide bonds, and it mediates IGF1-induced signaling. *IRS2* is the main effector of the proliferative signals triggered by IGF receptors (22). According to Western blot analysis, IGF1R and IRS2 are down-regulated in RSa cells by HuIFN-β and in F-IF^r cells by transfection with miR-431 precursors (Fig. 4A and B). These observations suggest that increased levels of miR-431 inhibit *IGF1R* and *IRS2* expression in RSa cells. In addition, we hypothesized that miR-431-mediated *IGF1R* and *IRS2* down-regulation would be accompanied by the inhibition of the PI3K-Akt and MAPK pathways. Indeed, HuIFN-β suppressed both signaling pathways in RSa cells (Fig. 5A). Transfection with miR-431 precursors inhibited the MAPK pathway in F-IF^r cells, although the PI3K-Akt pathway was not affected (Fig. 5C).

There are a number of clinical reports on the therapeutic use of HuIFN-β. For example, combination therapy with HuIFN-β and Ranimustive has been particularly useful for the treatment of malignant gliomas in Japan (23). In cases of newly diagnosed primary glioblastoma multiforme, HuIFN-β and temozolomide combination therapy is significantly associated with a favorable outcome (24). However, there are many hurdles facing the use of HuIFN-β as an anti-cancer agent, particularly for HuIFN-β resistant cancers. For example, NC65 tumors (a human renal cell carcinoma) transfected with recombinant HuIFN-β did not shrink and failed to undergo apoptosis (25). Thus, in clinical cases in which enhanced HuIFN-β sensitivity is desirable or in which resistance to HuIFN-β is encountered, the delivery of miR-431 precursors to the cancerous tissue, in combination with a PI3K inhibitor, may effectively suppress cancer growth.

In conclusion, our results demonstrate that miR-431, which is up-regulated by HuIFN-β in RSa cells, suppresses the IGF1R signaling pathway. Delivery of miR-431 and a PI3K inhibitor in a combination therapeutic approach may represent an effective strategy for the treatment of HuIFN-β resistant cancers.

Acknowledgments

The authors thank Mrs. Satomi Hasegawa for her excellent technical assistance. This research project was supported by the Ministry of Health, Labour and Welfare (Science Research Grants for intractable diseases in Japan; H22-intractable diseases-120), the Smoking Research Foundation, the Tsuchiya Foundation, the Kieikai Research Foundation, the Ministry of Health, Labour and Welfare for the Intractable Diseases Treatment Research Program, and the Japan Society for the Promotion of Science (Japan).

References

1. He L and Hannon GJ: MicroRNAs: small RNAs with a big role in gene regulation. Nat Rev Genet 5: 522-531, 2004.

2. Ambros V: The functions of animal microRNAs. Nature 431: 350-355, 2004.
3. Bartel DP: MicroRNAs: genomics, biogenesis, mechanism, and function. Cell 116: 281-297, 2004.
4. Lu J, Getz G, Miska EA, *et al*: MicroRNA expression profiles classify human cancers. Nature 2435: 834-838, 2005.
5. Kim SJ, Oh JS, Shin JY, *et al*: Development of microRNA-145 for therapeutic application in breast cancer. J Control Release (In press).
6. Bian HB, Pan X, Yang JS, Wang ZX and De W: Upregulation of microRNA-451 increases cisplatin sensitivity of non-small cell lung cancer cell line (A549). J Exp Clin Cancer Res 30: 20, 2011.
7. Tomimaru Y, Eguchi H, Nagano H, *et al*: MicroRNA-21 induces resistance to the anti-cancer effect of interferon-α/5-fluorouracil in hepatocellular carcinoma cells. Br J Cancer 103: 1617-1626, 2010.
8. Pfeffer LM: Mechanisms of interferon action. CRC Press, Boca Raton, FL, 1987.
9. Petska S, Langer AJ, Zoon K and Samuel C: Interferons and their action. Annu Rev Biochem 56: 727-777, 1987.
10. Taniguchi T and Takaoka A: The interferon-alpha/beta system in antiviral responses: a multimodal machinery of gene regulation by the IRF family of transcription factors. Curr Opin Immunol 14: 111-116, 2002.
11. Biron CA: Interferon alpha and beta as immune regulators - a new look. Immunity 14: 661-664, 2001.
12. Revel M and Chebath J: Interferon-activated genes. Trends Biochem Sci 11: 166-170, 1986.
13. Williams BR: Transcriptional regulation of interferon-stimulated genes. Eur J Biochem 200: 1-11, 1991.
14. Kogo R, Mimori K, Tanaka F, Komune S and Mori M: Clinical significance of miR-146a in gastric cancer cases. Clin Cancer Res 17: 4277-4284, 2011.
15. Saydam O, Senol O, Wurdinger T, *et al*: miRNA-7 atttenuation in Schwannoma tumors stimulates growth by upregulating three oncogenic signaling pathways. Cancer Res 71: 852-861, 2011.
16. Chou YT, Lin HH, Lien YU, *et al*: EGFR promotes lung tumorigenesis by activating miR-7 through a Ras/ERK/Myc pathway that targets the Ets2 transcriptional repressor ERF. Cancer Res 70: 8822-8831, 2010.
17. Giles KM, Barker A, Zhang PM, Epis MR and Leedman PJ: MicroRNA regulation of growth factor receptor signaling in human cancer cells. Methods Mol Biol 676: 147-163, 2011.
18. Guo C, Sah JF, Beard L, Willson JK, Markowitz SD and Guda K: The non-coding RNA, miR-126, suppresses the growth of neoplastic cells by targeting phosphatidylinositol 3-kinase signaling and is frequently lost in colon cancers. Gene Chromosomes Cancer 47: 939-946, 2008.
19. Kefas B, Godlewski J, Comeau L, *et al*: microRNA-7 inhibits the epidermal growth factor receptor and the Akt pathway and is down-regulated in glioblastoma. Cancer Res 68: 3566-3572, 2008.
20. La Rocca G, Badin M, Shi B, *et al*: Mechanism of growth inhibition by microRNA 145: the role of the IGF-I receptor signaling pathway. J Cell Physiol 220: 485-491, 2009.
21. Jiang L, Liu X, Chen Z, *et al*: MicroRNA-7 targets IGF1R (insulin-like growth factor 1 receptor) in tongue squamous cell carcinoma cells. Biochem J 432: 199-205, 2010.
22. Kwon J, Stephan S, Mukhopadhyay A, *et al*: Insulin receptor substrate-2 mediated insulin-like growth factor-I receptor over-expression in pancreatic adenocarcinoma through protein kinase Cδ. Cancer Res 69: 1350-1357, 2009.
23. Wakabayashi T, Hatano N, Kajita Y, *et al*: Initial and maintenance combination treatment with interferon-beta, MCNU (Ranimustine), and radiotherapy for patients with previously untreated malignant glioma. J Neurooncol 49: 57-62, 2000.
24. Motomura K, Natsume A, Kishida Y, *et al*: Benefits of interferon-β and temozolomide combination therapy for newly diagnosed primary glioblastoma with the unmethylated MGMT promoter. Cancer 117: 1721-1730, 2011.
25. Yamamoto K, Mizutani Y, Nakanishi H, *et al*: Significant anti-tumor activity of cationic multilamellar liposomes containing human interferon-β gene in combination with 5-fluorouracil against human renal cell carcinoma. Int J Oncol 33: 565-571, 2008.

Journal of Human Genetics (2011), 1–7

www.nature.com/jhg

ORIGINAL ARTICLE

Novel *PTCH1* mutations in Japanese Nevoid basal cell carcinoma syndrome patients: two familial and three sporadic cases including the first Japanese patient with medulloblastoma

Midori Fujii[1], Kazuma Noguchi[1], Masahiro Urade[1], Yukoh Muraki[2], Kuniyasu Moridera[1], Hiromitsu Kishimoto[1], Tomoko Hashimoto-Tamaoki[3,4] and Yoshiro Nakano[3]

Nevoid basal cell carcinoma syndrome (NBCCS), also known as Gorlin syndrome, is inherited in an autosomal dominant mode, and is characterized by a combination of developmental abnormalities and predisposition to form a variety of tumors. The hedgehog receptor *Patched1* (*PTCH1*) has been identified as the gene mutated in NBCCS. We analyzed *PTCH1* in two familial and three sporadic Japanese NBCCS cases, and identified five germline mutations in *PTCH1*. Two cases have a nonsense mutation (c.3058C>T and c.2760C>A), one a splice site mutation (c.584+2T>G), one a 1 bp insertion (c.2712_2713insA) and one a 1 bp deletion (c.980Gdel). All mutations induce truncation of the PTCH1 protein or could induce nonsense-mediated mRNA decay. The 11-year-old male patient with splice-site mutation (c.584+2T>G) had medulloblastoma (MB) at the age of 1 year. This is the first NBCCS patient with molecularly defined MB in Japan.
Journal of Human Genetics advance online publication, 3 March 2011; doi:10.1038/jhg.2011.2

Keywords: Gorlin syndrome; KCOT; medulloblastoma; mutation; Nevoid basal cell carcinoma syndrome (NBCCS); PTCH1

INTRODUCTION

Nevoid basal cell carcinoma syndrome (NBCCS; MIM 109400), also known as Gorlin syndrome or basal cell nevus syndrome, is a rare autosomal dominant disorder.[1,2] NBCCS is characterized by developmental defects, such as calcification of the falx celebri, multiple nevi, palmar and plantar pits and skeletal abnormality.[2,3] It is also known to predispose individuals to cancers, including basal cell carcinoma (BCC), keratocystic odontogenic tumor (KCOT), medulloblastoma (MB), rhabdomyosarcoma and benign tumors, such as ovarian and cardiac fibroma. The hedgehog (Hh) receptor, *Patched1* (*PTCH1*), the human homolog of *Drosophila* segment polarity gene *patched*, which is located at chromosome 9q22.3, has been identified as a gene responsible for NBCCS.[4–6] *PTCH1* spans 34 kb and consists of at least 23 exons. It encodes a 1447 amino acid protein with 12 potential hydrophobic membrane-spanning domains, intracellular amino-and carboxy-terminal regions and two large hydrophilic extracellular loops in which the Hh protein binds.[7,8] To date, nearly 300 mutations have been identified in *PTCH1*.[9] Among them, more than 150 germline mutations have been reported in NBCCS patients, including nonsense and missense mutations, insertions or deletions and splice site mutations. In addition to NBCCS cases, *PTCH1* mutations have also been reported in many malignant neoplasms, such as sporadic BCC, KCOT, MB, primitive neuroectodermal tumor, breast cancer, colon cancer and meningioma.[10,11] Nearly 90% of sporadic BCCs,[12] 10–20% of sporadic MBs[13] and approximately 30% of sporadic KCOTs[14] carry *PTCH1* loss-of-function mutations. KCOT and BCC are two major tumors that characteristically develop in NBCCS patients. However, MB and other cancers are rarely seen. It is currently unclear whether the locations of mutations within *PTCH1* are relevant to clinical manifestation in NBCCS. However, identification of mutations is very helpful for genetic counseling and for giving clinical advice because patients with mutations are at high risk of NBCCS.

Herein, we identified *PTCH1* mutations in two familial and three sporadic NBCCS cases whose first symptoms were KCOTs. One sporadic patient with a splice-site mutation had a history of MB. This is the first report of a molecularly defined Japanese NBCCS patient with MB. In addition, we have analyzed all data from molecularly defined Japanese NBCCS cases. Comparison among ethnically different NBCCS patients will be discussed.

MATERIALS AND METHODS

All analyses described below were approved by the Medical Ethics Board of Hyogo College of Medicine (No. 108) and Tokuyama Central Hospital. The patients and their parents gave informed consent to participate in this study.

[1]Department of Oral and Maxillofacial Surgery, Hyogo College of Medicine, Nishinomiya, Japan; [2]Division of Oral Surgery, Tokuyama Central Hospital, Shunan, Yamaguchi, Japan; [3]Department of Genetics, Hyogo College of Medicine, Nishinomiya, Japan and [4]Department of Clinical Genetics, Hyogo College of Medicine, Nishinomiya, Japan
Correspondence: Dr Y Nakano, Department of Genetics, Hyogo College of Medicine, 1-1 Mukogawa-cho, Nishinomiya, Hyogo 663-8501, Japan.
E-mail: y-nakano@hyo-med.ac.jp
Received 17 September 2010; revised 25 December 2010; accepted 27 December 2010

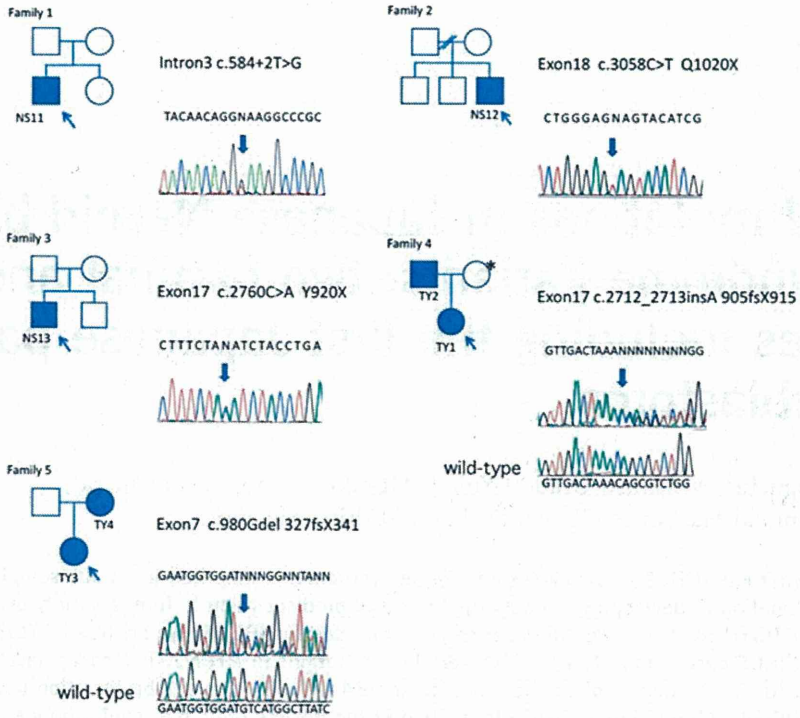

Figure 1 Pedigrees of five families with nevoid basal cell carcinoma syndrome, and electropherograms of the mutations. Filled symbols indicate patients. The arrows indicate the probands. The asterisk (*) represents a healthy individual whose DNA was sequenced.

Patients

We studied seven Japanese patients from five unrelated families who visited Hyogo College of Medicine or Tokuyama Central Hospital, Japan (Figure 1).

Family 1. An 11-year-old Japanese boy. He was born with congenital cleft lip and palate (Figure 2a), and was treated at the Department of Oral and Maxillofacial Surgery, Hyogo College of Medicine in 1996. During a series of treatments, MB was found (Figure 2c), and surgical resection and chemotherapy were performed. At the age of 11 years, he noticed pus discharge from the right second premolar of the mandible. Panoramic radiography and computed tomography revealed multiple cystic radiolucent areas with impacted teeth (Figure 2b). Moreover, ectopic calcification of the falx cerebri was also detected by computed tomography (Figure 2d). Broad forehead, highly arched eyebrows, ocular hypertelorism and palmar pits were present in this patient. Surgical resection of jaw cysts was performed. Histopathological diagnoses identified all lesions as KCOTs (Figure 2e).

Family 2. A 10-year-old Japanese boy. This patient felt pain in the left, second molar of the mandible, and consulted the Department of Oral and Maxillofacial Surgery, Hyogo College of Medicine. Panoramic radiography and computed tomography revealed multiple cystic radiolucent areas with impacted teeth. He underwent surgical resection of multiple jaw cysts, and histopathological diagnoses identified all lesions as KCOTs. He showed palmar and plantar pits, calcification of the falx cerebri and bifid ribs.

Family 3. A 47-year-old Japanese man. He underwent a series of surgical resections of multiple jaw cysts in the Department of Oral and Maxillofacial Surgery, Hyogo College of Medicine at the age of 36, 38 and 47 years. Histopathological diagnoses identified all lesions as KCOTs. BCCs were found in his skin at the age of 40 years and were surgically removed. He showed palmar and plantar pits, and calcification of the falx cerebri.

Family 4. The proband was a 9-year-old Japanese girl who showed multiple jaw cysts on panoramic radiography. She underwent an operation in the Division of Oral Surgery, Tokuyama Central Hospital. Histopathological diagnoses identified all lesions as KCOTs. She showed palmar and plantar pits and calcification of the falx cerebri. Her father, a 38-year-old Japanese, showed multiple jaw cysts, palmar and plantar pits, calcification of the falx cerebri and macrocephaly. Her mother was healthy.

Family 5. The proband was a 12-year-old Japanese girl who showed multiple jaw cysts on panoramic radiography. She underwent an operation in the Division of Oral Surgery, Tokuyama Central Hospital. Histopathological diagnoses identified all lesions as KCOTs. She showed palmar and plantar pits and calcification of the falx cerebri. Her mother, a 44-year-old Japanese, had KCOTs and showed calcification of the falx cerebri. Her father was healthy.

These cases were diagnosed as having NBCCS by the clinical criteria of Kimonis *et al.*[3] (Table 1).

DNA isolation, amplification and sequencing analysis

Genomic DNA from blood samples was extracted using the QIAamp DNA Blood Midi Kit (Qiagen, Hilden, Germany). All coding exons and intron–exon boundaries were amplified by PCR and sequenced. The primers used in this study have been previously described.[15] PCR was carried out in a total reaction volume of 50 µl, containing 100 ng genomic DNA, 1 U Primer STAR HS DNA polymerase (TaKaRa, Ohtsu, Japan), 200 µM dNTPs and 0.2 µM of each primer. Amplification was carried out for 40 cycles of 98 °C for 10 s, 55 °C for 5 s and 72 °C for 60 s. Amplified products were purified using the MinElute PCR Purification Kit (Qiagen). Sequencing was performed using a BigDye Terminator v3.1 Cycle Sequencing Kit (Applied Biosystems, Foster City, CA, USA) and a 3130xl Genetic Analyzer (Applied Biosystems), according to the manufacturer's instructions.

For analysis of aberrant splicing, total RNA was extracted from cell line, ImNBCCS-KCOT (KCOT-derived cell line from patient NS11: Noguchi K, manuscript in preparation), using the QIAamp RNA Blood Mini Kit (Qiagen) and subjected to RT-PCR using a Cells-to-cDNA II Kit (Applied Biosystems). The forward primer for exon 3 was 5′-TTATACTCGCCAGAAGATTGGAGA AGA-3′, and the reverse primer for exon 6 was 5′-GTCCATGTAACCATGACCA

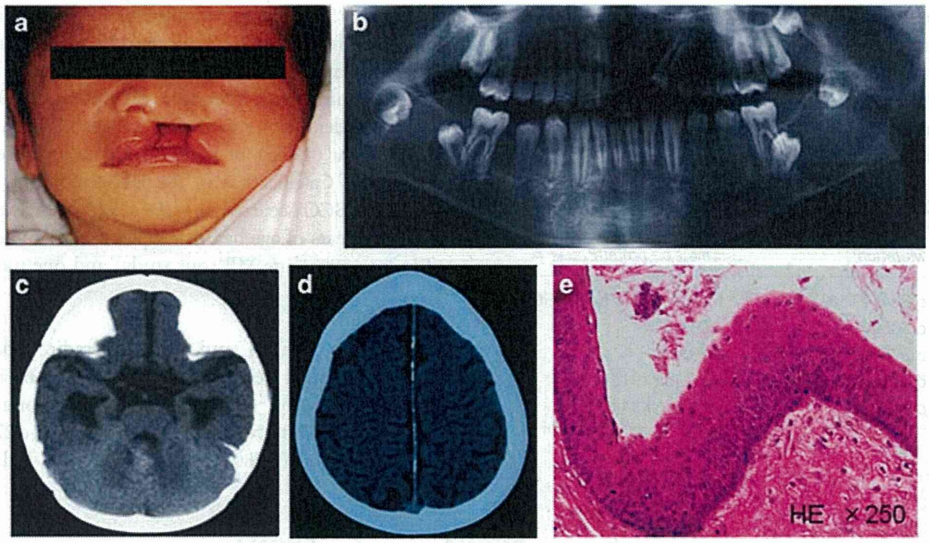

Figure 2 Patient NS11, an 11-year-old boy. (**a**) Congenital cleft lip and palate. (**b**) Panoramic radiograph reveals multiple cystic radiolucent areas with impacted teeth (age 11 years). (**c**) CT showed medulloblastoma in the brain (age 1 years). (**d**) Ectopic calcification of the falx cerebri (age 11 years). (**e**) Hematoxylin and eosin (HE) staining shows keratinized squamous epithelium, indicating a keratocystic odontogenic tumor (age 11 years).

Table 1 Characteristics of the patients in this study

	Patient (age in years)						
Diagnostic criteria according to Kimonis et al.[3]	*NS11 (11)*	*NS12 (10)*	*NS13 (47)*	*TY1 (9)*	*TY2 (38)*	*TY3 (12)*	*TY4 (44)*
Major symptoms							
Basal cell carcinoma (more than two or under the age of 20 years)	–	–	+	–	–	–	–
Keratocystic odontogenic tumor	+	+	+	+	+	+	+
Palmar and plantar pits (more than three)	+	+	+	+	+	+	–
Ectopic calcification of the falx cerebri	+	+	+	+	+	+	+
First-degree relative with NBCCS	–	–	–	–	+	–	+
Minor symptoms							
Macrocephaly (after correction for height)	–	–	–	–	+	–	–
Congenital malformation	+	–	–	–	–	–	–
Other skeletal abnormalities	–	–	–	–	–	–	–
Abnormality in radiological examination	–	–	–	–	–	–	–
Ovarian fibroma	–	–	–	–	–	–	–
Medulloblastoma	+	–	–	–	–	–	–

ACCTCAG-3′. Amplified products were gel purified and sequenced as described above.

Data analysis of Japanese NBCCS patients

Data from molecularly defined Japanese NBCCS patients were obtained from published papers. Suspected NBCCS patients, who had not been molecularly defined, were excluded in this analysis. All patients were analyzed based on major diagnostic criteria, such as BCC, KCOT, palmar and plantar pits, calcification of the falx cerebri and various tumors.

RESULTS

Sequencing analysis revealed *PTCH1* mutations in all NBCCS patients (Figure 1, Table 2). The mutations in families 1, 2, 4 and 5 were novel, and the mutation in family 3 was previously reported in a KCOT sample from a Brazilian NBCCS patient.[16] We found a mutation at a *PTCH1* splice donor site in patient NS11, therefore, we analyzed *PTCH1* mRNA using cells derived from a KCOT from NS11. Sequence analysis of DNA derived from KCOT cells and peripheral blood of NS11 showed identical patterns. Therefore, a cell line was derived from the NS11 KCOT and neither additional mutations nor evidence of loss of heterozygosity in *PTCH1* were found in these cells. To analyze the splicing events, total RNA was extracted from NS11-derived cells and RT-PCR was performed using a pair of primers located in exon 3 and exon 6 (Figure 3d). RT-PCR produced two bands (Figure 3a), which were sequenced separately (Figures 3b and c). The short transcript, transcript 1, consisted of wild-type sequences (Figure 3b). The longer fragment revealed that this mutation activated a cryptic splice site in intron 3, resulting in a 37 bp insertion of intronic sequence into the mRNA (Figures 3c and d). This insertion induced a frame shift and termination after 58 additional amino acids. This additional sequence did not show obvious homology to any other known protein.

In families 2 and 3, the mutations created stop codons (Table 2). In families 4 and 5, the mutations caused frame shifts, resulting in stop codons after 11 and 15 amino acids, respectively.

The spectrum of *PTCH1* mutations in Japanese NBCCS patients was analyzed based on the literature.[15,17–28] Table 3 summarizes the spectrum of *PTCH1* mutations and phenotypes of Japanese NBCCS patients. Overall 56 subjects who fulfilled the criteria for NBCCS were analyzed. There were 31 men and 25 women, ranging in age from 0 to 71 years (average 26.3 years). Mutations were scattered throughout the entire gene. Therefore, there is no mutational hot spot and also no founder effect for NBCCS in Japan. Patients with KCOTs represented 87.3% (48/55) of patients. Pits were observed in 43/53 (81.1%) of cases. Calcification of the falx cerebri was seen in 39/50 (78.0%) of cases. BCC occurred in 14/56 (25.0%) of cases. 8/15 (53.3%) of cases over 40 years of age had developed a BCC. Other cancers were reported in two cases, one MB (our study) and one meningioma.

Table 2 Germline mutations in the *PTCH1* gene

Family	*Exon*	*Mutation*[a]	*Effect on protein*[b]
1	Intron 3	c.584+2T>G	Insertions and frameshift
2	Exon 18	c.3058C>T	p.Q1020X
3	Exon 17	c.2760C>A	p.Y920X
4	Exon 17	c.2712_2713insA	p.R905fsX915
5	Exon 7	c.980Gdel	p.R327fsX341

[a]NM_000264.
[b]NP_000255.

DISCUSSION

We analyzed two familial and three sporadic Japanese NBCCS patients, and identified germline *PTCH1* mutations in all patients: one splice site mutation (c.584+2T>G), two nonsense mutations (c.3058C>T and c.2760C>A), one 1 bp insertion (c.2712_2713insA) and one 1 bp deletion (c.980Gdel). All mutations induce premature

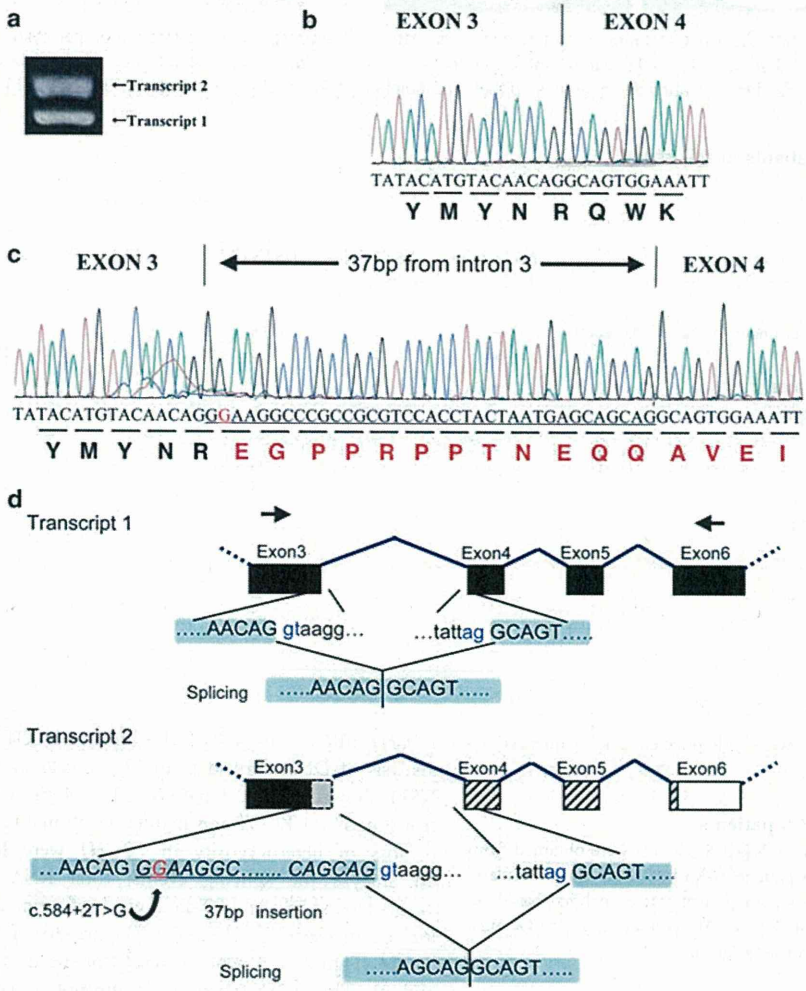

Figure 3 The *PTCH1* mutation found in patient NS11 (c.584+2T>G) induced aberrant splicing. (**a**) Analysis of the splice donor mutation in NS11. RT-PCR was carried out using RNAs from NS11-derived cells. Primers are illustrated as black arrows in (**d**). Gel electrophoresis of RT-PCR products produces two bands. (**b**, **c**) Sequence analysis of the two RT-PCR products. Lower fragment (transcript 1) indicated a normal splicing event (**b**). The upper fragment (transcript 2) showed that the c.584+2T>G mutation led to the activation of a cryptic splice site in intron 3, resulting in the insertion of a 37 bp intronic sequence into the mRNA (**c**). (**d**) Schematic representation of the splicing events induced by the c.584+2T>G mutation. One allele produced normal mRNAs (transcript 1). The other mutated allele produced mRNAs with a 37 bp insertion resulting in a frame shift mutation. Black boxes indicate coding exons. Gray box indicates intronic sequence inserted into the mRNA. Hatched areas show frame-shifted regions. White represents non-coding sequence.

Table 3 PTCH1 mutations and clinical features of Japanese nevoid basal cell carcinoma syndrome patients

Type of mutation	*Exon*	*Nucleotide change*	*Age (in years)*	*Sex*	*BCC*	*KCOT*	*Pits*	*Calcification of falx cerebri*	*Other cancer*	*Reference*
2 bp deletion	2	c.239_240delGA	18	M	–	+	+	+	–	Takahashi *et al.*[15]
Nonsense	2	c.279C>A	16	F	–	+	+	+	–	Minami *et al.*[17]
Missense	2	c.328G>T	19	M	–	+	+	+	–	Tanioka *et al.*[22]
Missense	2	c.328G>T	43	F	–	+	+	–	–	Tanioka *et al.*[22]
1 bp deletion	3	c.459delT	27	F	+	+	+	+	–	Nagao *et al.*[21]
Splicing	3	c.584G>A	61	M	+	+	+	–	–	Nagao *et al.*[21]
Splicing	intron 3	c.584+2T>G	11	M	–	+	+	+	Medulloblastoma	This study
1 bp deletion	6	c.865delC	29	M	–	+	+	+	–	Tanioka *et al.*[22]
1 bp deletion	6	c.912delC	18	F	–	+	+	+	–	Fujii *et al.*[19]
1 bp deletion	6	c.912delC	16	F	–	+	+	+	–	Fujii *et al.*[19]
Splicing	intron6	c.945+5G>T	5	M	–	–	+	-	–	Fujii *et al.*[19]
1 bp deletion	7	c.980Gdel	12	F	–	+	+	+	–	This study
1 bp deletion	7	c.980Gdel	44	F	–	+	–	+	–	This study
Splicing	intron7	c.1067+1G>C	16	M	–	+	–	+	–	Sasaki *et al.*[27]
58 bp duplication	8	c.1138_1195dup	12	M	–	+	+	+	–	Takahashi *et al.*[15]
Missense	8	c.1162A>T	70	F	+	–	NR	NR	–	Ogata *et al.*[18]
Nonsense	8	c.1196G>A	10	F	–	+	-	+	–	Takahashi *et al.*[15]
Nonsense	8	c.1196G>A	0	F	–	–	-	NR	–	Takahashi *et al.*[15]
1 bp insertion	9	c.1261insT	17	F	–	+	+	+	–	Fujii *et al.*[19]
4 bp duplication	10	c.1416_1419dupTGGC	3	M	–	–	+	+	–	Nagao *et al.*[21], Tachi *et al.*[24], Honma *et al.*[25]
1 bp deletion	10	1427delT	15	F	–	+	+	+	–	Sasaki *et al.*[28]
Missense	11	c.1526G>A	66	M	+	+	+	+	–	Fujii *et al.*[19]
Missense	12	c.1660A>C	44	M	–	+	–	+	–	Tanioka *et al.*[22]
2 bp deletion	12	c.1670_1671delCA	18	F	–	+	+	+	–	Takahashi *et al.*[15]
2 bp deletion	12	c.1670_1671delCA	46	F	–	+	+	+	–	Takahashi *et al.*[15]
1 bp deletion	14	c.2011delC	59	F	+	+	+	+	–	Fujii *et al.*[19]
1 bp deletion	14	c.2029delA	23	F	–	+	+	+	–	Takahashi *et al.*[15]
1 bp deletion	15	c.2395delT	29	M	+	+	+	+	–	Minami *et al.*[17]
1 bp deletion	15	c.2395delT	NR	M	+	+	–	+	–	Minami *et al.*[17]
1 bp deletion	15	c.2395delT	NR	M	+	+	–	+	–	Minami *et al.*[17]
1 bp duplication	15	c.2454dupA	28	M	–	+	+	+	–	Tanioka *et al.*[22]
1 bp deletion	16	c.2613delC	50	F	+	+	NR	NR	Meningioma	Tate *et al.*[20]
1 bp deletion	16	c.2613delC	NR	F	+	NR	NR	NR	–	Tate *et al.*[20]
1 bp insertion	17	c.2712_2713insA	9	F	–	+	+	+	–	This study
1 bp insertion	17	c.2712_2713insA	38	M	–	+	+	+	–	This study
1 bp insertion	17	c.2724_2725insT	26	F	–	+	+	+	–	Nagao *et al.*[21]
Missense	17	c.2760C>A	40	M	+	+	+	+	–	This study
22 bp deletion and 9 bp insertion	17	c.2785_2806del22ins9	20	M	–	+	+	+	–	Tanioka *et al.*[22]
Nonsense	18	c.2908G>T	71	M	+	-	+	+	–	Tanioka *et al.*[22]
1 bp deletion	18	c.3016delC	46	F	+	+	+	-	–	Tanioka *et al.*[22]
Missense	18	c.3058C>T	10	M	–	+	+	+	–	This study
2 bp duplication	18	c.3130_3131dupGC	3	M	–	+	+	–	–	Nagao *et al.*[21]
2 bp duplication	18	c.3130_3131dupGC	37	F	–	+	+	–	–	Nagao *et al.*[21]
4 bp duplication	20	c.3325_3328dupGGCG	23	M	–	+	+	+	–	Sasaki *et al.*[27]
2 bp deletion	20	c.3364_3365 delAT	10	M	–	+	+	-	–	Nagao *et al.*[21]
Missense	20	c.3398C>T	47	F	–	+	+	+	–	Otsubo *et al.*[26]
Missense	20	c.3398C>T	22	M	–	+	+	+	–	Otsubo *et al.*[26]
Missense	20	c.3398C>T	19	F	–	+	+	+	–	Otsubo *et al.*[26]
Missense	20	c.3398C>T	17	M	–	+	+	–	–	Otsubo *et al.*[26]
165 kb deletion	1–23		10	M	–	+	–	–	–	Fujii *et al.*[23]
165 kb deletion	1–23		43	F	–	–	–	–	–	Fujii *et al.*[23]
1.2 Mb deletion	1–23		12	M	–	+	+	+	–	Takahashi *et al.*[15]
1.2 Mb deletion	1–23		40	M	–	+	+	NR	–	Takahashi *et al.*[15]
1.2 Mb deletion	1–23		8	M	–	+	+	NR	–	Takahashi *et al.*[15]
5.3 Mb deletion	1–23		8	M	–	–	+	–	–	Fujii *et al.*[23]
11 Mb deletion	1–23		12	M	+	+	–	+	–	Fujii *et al.*[23]
			ave.	M:F	14/56	48/55	43/53	39/50	2/55	
			26.3	31:25	25.0%	87.3%	81.1%	78.0%	3.6%	

Abbreviations: ave., average; BCC, basal cell carcinoma; F, female; KCOT, keratocystic odontogenic tumor; M, male; NR, not reported.

Table 4 Comparison of frequency of major criteria in NBCCS patients among seven studies

	UK; Evans et al.[29]	*Australia; Shanley et al.*[30]	*USA; Kimonis et al.*[3]	*Italy; Lo Muzio et al.*[31]	*Korea; Ahn et al.*[32]	*Iran; Habibi et al.*[33]	*Japan; this study*
Patients	84	118	105	37	33	19	56
Age (in years)	NR	35	NR	31.4	21.2	32.	26.3
Male/female	NR	51:67	48:57	16:21	16:17	10:9	31:25
Major criteria number (%)							
BCCs	33/70 (47)	90/118 (76)	71/90 (80)[a] 5/13 (38)[b]	11/37 (30)	5/33 (15)	8/19 (42)	14/56 (25)
>20 years	33/45 (73)	71/84 (85)	58/64 (91)[a]	2/25 (8)[c]	NR	5/10 (50)	10/26 (38)
>40 years	19/21 (90)	35/37 (95)	34/35 (97)[a]	9/12 (75)	NR	2/4 (50)	8/15 (53)
KCOTs	46/70 (66)	85/113 (75)	78/105 (74)	34/37 (92)	30/33 (91)	19/19 (100)	48/55 (87)
>20 years	37/45 (82)	66/82 (80)	60/74 (81)	NR	NR	10/10 (100)	21/26 (81)
>40 years	19/21 (90)	25/35 (71)	29/38 (76)	NR	NR	4/4 (100)	11/15 (73)
Pits	50/70 (71)	82/103 (80)	89/102 (87)	13/37 (35)	22/33 (67)	14/19 (74)	43/53 (81)
Calcification	NR	81/88 (92)	53/82 (65)	26/37 (70)	7/33 (21)	17/19 (89)	39/50 (78)

Abbreviations: BCC, basal cell carcinoma; KCOT, keratocystic odontogenic tumor; NR, not reported.
[a]White.
[b]African American.
[c]0–40 years.

termination of the PTCH1 protein or could induce nonsense-mediated mRNA decay.

A point mutation in intron 3 (c.584+2T>G) of *PTCH1* was detected in patient NS11. RT-PCR analysis revealed that at least two transcripts were generated from this region (Figure 3a). Sequence analysis indicated that the short transcript, transcript 1, consisted of wild-type sequences (Figure 3b), whereas the long transcript, transcript 2, consisted of a mutated sequence (Figure 3c). These data suggested that the long transcript was not the product of a normal alternative splicing event and that c.584+2T>G generated a cryptic splice site in intron 3, resulting in the insertion of 37 extra bases into the mRNA. This activated splice site conformed to the authentic GT-AG rule. Interestingly, a very similar, but not identical mutation, which generates an identical 37-bp insertion, has been reported.[21] In that case, the mutation, c.584G>A, was in the exon, but affected the splice donor sequence and induced aberrant splicing. The cryptic splice site generated by c.584G>A was identical to that generated by c.584+2T>G.

Patient NS11 showed a complicated cleft lip and palate with MB (Figure 2). In NBCCS, the morbidity rate of cleft lip and palate is approximately 5%, which is the same as that of MB.[3,29,30] Therefore, this is a very rare case. His clinical manifestation was severe, but none of his family exhibited NBCCS symptoms; therefore, this mutation seems to be *de novo*. This is the first report of a Japanese NBCCS patient with MB. *PTCH1* mutations in sporadic MBs are scattered throughout the entire gene,[9] similar to that of NBCCS cases, indicating no correlation between the position of the mutations and the observed phenotype. His KCOT-derived cells showed neither extra mutations nor evidence of loss of heterozygosity, at least in the *PTCH1*-coding region. Therefore, additional alterations, in addition to that in observed *PTCH1*, must be involved in this KCOT formation.

Clinical manifestations in NBCCS individuals have been reported in different ethnic groups.[3,29–33] Comparison of the frequencies of major phenotypes in NBCCS, such as BCCs, KCOTs, palmar or plantar pits and calcification of the falx cerebri are listed in Table 4. Obvious differences were found in the onset of BCCs. In Caucasian NBCCS patients, more than 70% (over the age of 20 years) or 90% (over the age of 40 years) of patients developed BCC.[3,29,30] Kimonis *et al.*[3] estimated that the probability of developing BCCs was approximately 90% in Caucasians and 40% in African-Americans by the age of 35 years. In contrast, BCCs developed in only 38% (over the age of 20 years) and 53% (over the age of 40 years) of Japanese patients. On the other hand, KCOT was found in more than 80% (over the age of 20 years) in all populations. These data suggested that allelic loss of *PTCH1* has different consequences in different genetic backgrounds and in different tissues. The analysis of molecules involved in these differences will help to prevent or delay the onset of BCCs.

CONFLICT OF INTEREST

The authors declare no conflict of interest.

ACKNOWLEDGEMENTS

We thank the patients and their families for making this study possible. This work was supported, in part, by the Research fund of the Hyogo College of Medicine.

1 Gorlin, R. J. Nevoid basal cell carcinoma (Gorlin) syndrome: unanswered issues. *J. Lab. Clin. Med.* **134,** 551–552 (1999).
2 Cohen, Jr M. M. Nevoid basal cell carcinoma syndrome: molecular biology and new hypotheses. *Int. J. Oral. Maxillofac. Surg.* **28,** 216–223 (1999).
3 Kimonis, V. E., Goldstein, A. M., Pastakia, B., Yang, M. L., Kase, R., DiGiovanna, J. J. *et al.* Clinical manifestations in 105 persons with nevoid basal cell carcinoma syndrome. *Am. J. Med. Genet.* **69,** 299–308 (1997).
4 Johnson, R. L., Rothman, A. L., Xie, J., Goodrich, L. V., Bare, J. W., Bonifas, J. M. *et al.* Human homolog of patched, a candidate gene for the basal cell nevus syndrome. *Science* **272,** 1668–1671 (1996).
5 Hahn, H., Wicking, C., Zaphiropoulous, P. G., Gailani, M. R., Shanley, S., Chidambaram, A. *et al.* Mutations of the human homolog of Drosophila patched in the nevoid basal cell carcinoma syndrome. *Cell* **85,** 841–851 (1996).
6 Unden, A. B., Holmberg, E., Lundh-Rozell, B., Ståhle-Bäckdahl, M., Zaphiropoulos, P. G., Toftgård, R. *et al.* I. Mutations in the human homologue of Drosophila patched (PTCH) in basal cell carcinomas and the Gorlin syndrome: different *in vivo* mechanisms of PTCH inactivation. *Cancer Res.* **56,** 4562–4565 (1996).
7 Stone, D. M., Hynes, M., Armanini, M., Swanson, T. A., Gu, Q., Johnson, R. L. *et al.* The tumour-suppressor gene patched encodes a candidate receptor for Sonic hedgehog. *Nature* **384,** 129–134 (1996).
8 Marigo, V., Davey, R. A., Zuo, Y., Cunningham, J. M. & Tabin, C. J. Biochemical evidence that patched is the Hedgehog receptor. *Nature* **384,** 176–179 (1996).
9 Lindström, E., Shimokawa, T., Toftgård, R. & Zaphiropoulos, P. G. PTCH mutations: distribution and analyses. *Hum. Mutat.* **27,** 215–219 (2006).
10 Wolter, M., Reifenberger, J., Sommer, C., Ruzicka, T. & Reifenberger, G. Mutations in the human homologue of the Drosophila segment polarity gene patched (PTCH) in

sporadic basal cell carcinomas of the skin and primitive neuroectodermal tumors of the central nervous system. *Cancer Res.* **57,** 2581–2585 (1997).
11 Xie, J., Johnson, R. L., Zhang, X., Bare, J. W., Waldman, F. M., Cogen, P. H. *et al.* Mutations of the PATCHED gene in several types of sporadic extracutaneous tumors. *Cancer Res.* **57,** 2369–2372 (1997).
12 Epstein, E. H. Basal cell carcinomas: attack of the hedgehog. *Nat. Rev. Cancer* **8,** 743–754 (2008).
13 Teglund, S. & Toftgard, R. Hedgehog beyond medulloblastoma and basal cell carcinoma. *Biochim Biophys Acta* **1805,** 181–208 (2010).
14 Pan, S., Dong, Q., Sun, L. S. & Li, T. J. Mechanisms of inactivation of PTCH1 gene in nevoid basal cell carcinoma syndrome: modification of the two-hit hypothesis. *Clin. Cancer Res.* **16,** 442–450 (2010).
15 Takahashi, C., Kanazawa, N., Yoshikawa, Y., Yoshikawa, R., Saitoh, Y., Chiyo, H. *et al.* Germline PTCH1 mutations in Japanese basal cell nevus syndrome patients. *J. Hum. Genet.* **54,** 403–408 (2009).
16 Barreto, D. C., Gomez, R. S., Bale, A. E., Boson, W. L. & De Marco, L. PTCH gene mutations in odontogenic keratocysts. *J. Dent. Res.* **79,** 1418–1422 (2000).
17 Minami, M., Urano, Y., Ishigami, T., Tsuda, H., Kusaka, J. & Arase, S. Germline mutations of the PTCH gene in Japanese patients with nevoid basal cell carcinoma syndrome. *J. Dermatol. Sci.* **27,** 21–26 (2001).
18 Ogata, K., Ikeda, M., Miyoshi, K., Yamamoto, Y., Yamamoto, T., Osaki, T. *et al.* Naevoid basal cell carcinoma syndrome with a palmar epidermoid cyst, milia and maxillary cysts. *Br. J. Dermatol.* **145,** 508–509 (2001).
19 Fujii, K., Kohno, Y., Sugita, K., Nakamura, M., Moroi, Y., Urabe, K. *et al.* Mutations in the human homologue of Drosophila patched in Japanese nevoid basal cell carcinoma syndrome patients. *Hum. Mutat.* **21,** 451–452 (2003).
20 Tate, G., Li, M., Suzuki, T. & Mitsuya, T. A new germline mutation of the PTCH gene in a Japanese patient with nevoid basal cell carcinoma syndrome associated with meningioma. *Jpn. J. Clin. Oncol.* **33,** 47–50 (2003).
21 Nagao, K., Togawa, N., Fujii, K., Uchikawa, H., Kohno, Y., Yamada, M. *et al.* Detecting tissue-specific alternative splicing and disease-associated aberrant splicing of the PTCH gene with exon junction microarrays. *Hum. Mol. Genet.* **14,** 3379–3388 (2005).
22 Tanioka, M., Takahashi, K., Kawabata, T., Kosugi, S., Murakami, K., Miyachi, Y. *et al.* Germline mutations of the PTCH gene in Japanese patients with nevoid basal cell carcinoma syndrome. *Arch. Dermatol. Res.* **296,** 303–308 (2005).
23 Fujii, K., Ishikawa, S., Uchikawa, H., Komura, D., Shapero, M. H., Shen, F. *et al.* High-density oligonucleotide array with sub-kilobase resolution reveals breakpoint information of submicroscopic deletions in nevoid basal cell carcinoma syndrome. *Hum. Genet.* **122,** 459–466 (2007).
24 Tachi, N., Fujii, K., Kimura, M., Seki, K., Hirakai, M. & Miyashita, T. New mutation of the PTCH gene in nevoid basal-cell carcinoma syndrome with West syndrome. *Pediatr. Neurol.* **37,** 363–365 (2007).
25 Honma, M., Ohishi, Y., Uehara, J., Ibe, M., Kinouchi, M., Ishida-Yamamoto, A. *et al.* A novel PTCH1 mutation in a patient of nevoid basal cell carcinoma syndrome. *J. Dermatol. Sci.* **50,** 73–75 (2008).
26 Otsubo, S., Honma, M., Asano, K., Takahashi, H. & Iizuka, H. A novel germ-line mutation of PTCH1 gene in a Japanese family of nevoid basal cell carcinoma syndrome: are the palmoplantar pits associated with true basal cell carcinoma? *J. Dermatol. Sci.* **51,** 144–146 (2008).
27 Sasaki, R., Saito, K., Watanabe, Y., Takayama, Y., Fujii, K., Agawa, K. *et al.* Nevoid basal cell carcinoma syndrome with cleft lip and palate associated with the novel PTCH gene mutations. *J. Hum. Genet.* **54,** 398–402 (2009).
28 Sasaki, R., Miyashita, T., Matsumoto, N., Fujii, K., Saito, K. & Ando, T. Multiple keratocystic odontogenic tumors associated with nevoid basal cell carcinoma syndrome having distinct PTCH1 mutations: a case report. *Oral Surg. Oral Med. Oral Pathol. Oral Radiol. Endod.* **110,** e41–e46 (2010).
29 Evans, D. G., Ladusans, E. J., Rimmer, S., Burnell, L. D., Thakker, N. & Farndon, P. A. Complications of the naevoid basal cell carcinoma syndrome: results of a population based study. *J. Med. Genet.* **30,** 460–464 (1993).
30 Shanley, S., Ratcliffe, J., Hockey, A., Haan, E., Oley, C., Ravine, D. *et al.* Nevoid basal cell carcinoma syndrome: review of 118 affected individuals. *Am. J. Med. Genet.* **50,** 282–290 (1994).
31 Lo Muzio, L., Nocini, P. F., Savoia, A., Consolo, U., Procaccini, M., Zelante, L. *et al.* Nevoid basal cell carcinoma syndrome. Clinical findings in 37 Italian affected individuals. *Clin. Genet.* **55,** 34–40 (1999).
32 Ahn, S. G., Lim, Y. S., Kim, D. K., Kim, S. G., Lee, S. H. & Yoon, J. H. Nevoid basal cell carcinoma syndrome: a retrospective analysis of 33 affected Korean individuals. *Int J Oral Maxillofac Surg.* **33,** 458–462 (2004).
33 Habibi, A. & Jafarzadeh, H. Nevoid basal cell carcinoma syndrome: a 17-year study of 19 cases in Iranian population (1991–2008). *J. Oral Pathol. Med.* **39,** 677–680 (2010).

RADIATION RESEARCH 176, 732–742 (2011)
0033-7587/11 $15.00

DOI: 10.1667/RR2561.1

Extracellular Recombinant Annexin II Confers UVC-Radiation Resistance and Increases the Bcl-xL to Bax Protein Ratios in Human UVC-Radiation-Sensitive Cells

Kazuko Kita,[a,1,2] Katsuo Sugita,[b,1] Shi-Ping Chen,[a,1] Toshikazu Suzuki,[a,c] Shigeru Sugaya,[a] Takeshi Tanaka,[a] Yuan-Hu Jin,[a] Tetsuo Satoh,[a] Xiao-Bo Tong[d] and Nobuo Suzuki[a,2]

[a] *Department of Environmental Biochemistry, Graduate School of Medicine, Chiba University, Inohana, Chuou-ku, Chiba 260-8670, Japan;* [b] *Department of Clinical Medicine, Faculty Education, Chiba University, Yayoi-cho, Inage-ku, Chiba 263-8522, Japan;* [c] *Department of Health and Nutrition, Wayo Women's University, Konodai, Ichikawa 272-8533, Japan; and* [d] *Department of Physiology, Faculty of Basic Medical Sciences, Chengde Medical University, Chengde 067000, P.R. China*

Kita, K., Sugita, K., Chen, S. P., Suzuki, T., Sugaya, S., Tanaka, T., Jin, Y. H., Satoh, T., Tong, X. B. and Suzuki, N. Extracellular Recombinant Annexin II Confers UVC-Radiation Resistance and Increases the Bcl-xL to Bax Protein Ratios in Human UVC-Radiation-Sensitive Cells. *Radiat. Res.* 176, 732–742 (2011).

In this study, we found that refractoriness to ultraviolet (UVC) light-induced cell death was increased in UVC-radiation-sensitive cells derived from Cockayne syndrome patients when the cells were precultured in medium supplemented with recombinant annexin II (rANX II). In CS3BES cells, an immortal cell line derived from Cockayne syndrome patients, the rANX II supplementation-induced UVC-radiation resistance was suppressed by treatment with an anti-annexin II antibody and EGTA. The amount of biotinylated annexin II on the cell surface increased in the rANX II-supplemented cells but did not increase in the cells that were cotreated with rANX II and EGTA. The capacity to remove UVC-radiation-damaged DNA, (6-4) photoproducts and cyclobutane pyrimidine dimers, was the same in cells that were precultured with rANX II and in control cells that did not receive rANX II supplementation. The rANX II supplementation-induced UVC-radiation resistance was also observed in nucleotide excision repair-deficient cells and xeroderma pigmentosum group A-downregulated cells. The Bcl-xL to Bax protein ratios, an index of survival activity in cells exposed to lethal stresses, were increased in the cells that had been precultured in rANX II for 24 h prior to UVC irradiation. Treatment with a phosphatidylinositol 3-kinase inhibitor suppressed the increased UVC-radiation resistance and Bcl-xL to Bax ratios in the cells with rANX II supplementation. Furthermore, downregulation of Bcl-xL by siRNA transfection also suppressed the UVC-radiation resistance that was induced by rANX II supplementation. These results suggest that the increase in the Bcl-xL to Bax ratios may be associated with enhanced resistance to UVC-radiation-induced cell death. © 2011 by Radiation Research Society

INTRODUCTION

Cockayne syndrome (CS) is a rare autosomal recessive disease characterized by acute sun sensitivity, cachectic dwarfism, skeletal abnormalities, pigmentary retinal degeneration, and progressive neurological defects including dementia (*1*). Cultured cells from CS patients (CS cells) are hypersensitive to the cell-killing effects of radiation, particularly 254-nm wavelength ultraviolet light (UVC radiation) (*2*). The molecular mechanisms underlying this hypersensitivity have been studied extensively, and the details of the abnormalities in DNA metabolism in CS cells have been clarified (*3*). However, there is no proposed method to reduce the cellular UV-radiation hypersensitivity effectively in the cells of CS patients.

UVC radiation does not reach the Earth, while UVB radiation (280–320 nm) and UVA radiation (320–400 nm) do. UVC and UVB radiation cause dimeric pyrimidine damage to DNA, and UVB and UVA radiation cause oxidative damage to DNA. In our study, we used UVC radiation as a DNA-damaging agent to elucidate responses of human cells to the DNA-damaging effects of UV radiation. Human cells may possess common mechanisms to protect against the DNA-damaging effects of UVB and UVC radiation, and we recently determined that a cellular protective mechanism against UVC radiation can also function to protect human cells from UVB radiation (unpublished data).

We previously found that CS fibroblasts that were cultured in medium containing human interferon (HuIFN)-β and subsequently irradiated with UVC radiation exhibit

Note. The online version of this article (DOI: 10.1667/RR2561.1) contains supplementary information that is available to all authorized users.

[1]Equally contributing authors.

[2]Addresses for correspondence: Department of Environmental Biochemistry, Graduate School of Medicine, Chiba University, 1-8-1 Inohana, Chuo-ku, Chiba 260-8670, Japan; e-mail: kita@faculty.chiba-u.jp; Department of Environmental Biochemistry, Graduate School of Medicine, Chiba University, 1-8-1 Inohana, Chuo-ku, Chiba 260-8670, Japan; e-mail: nobuo@faculty.chiba-u.jp.